PLOS ONE

RESEARCH ARTICLE

Genetic resistance to DEHP-induced transgenerational endocrine disruption

Ludwig Stenz[1]*, Rita Rahban[1], Julien Prados[2,3], Serge Nef[1], Ariane Paoloni-Giacobino[1]

1 Department of Genetic Medicine and Development, Geneva University, Medicine Faculty, Geneva, Switzerland, **2** Department of Microbiology and Molecular Medicine, Geneva University, Medicine Faculty, Geneva, Switzerland, **3** Department of Neuroscience, Geneva University, Medicine Faculty, Geneva, Switzerland

* ludwig.stenz@unige.ch

OPEN ACCESS

Citation: Stenz L, Rahban R, Prados J, Nef S, Paoloni-Giacobino A (2019) Genetic resistance to DEHP-induced transgenerational endocrine disruption. PLoS ONE 14(6): e0208371. https://doi.org/10.1371/journal.pone.0208371

Editor: Joël R. Drevet, Universite Clermont Auvergne, FRANCE

Received: November 13, 2018

Accepted: May 15, 2019

Published: June 10, 2019

Data Availability Statement: The data have also been deposited in the NCBI Gene Expression Omnibus as GEO series accession number GSE107839. Files were converted by NCBI to Sequence Read Archive (SRA) files. We reused 10 samples from the previous GEO series accession number GSE86837. The MBD-seq data were reused from the GEO series accession number GSE67159. The analysis of SNPs impacting on hormonal binding motifs in the function of strain-specific RNA responses in male germ cells was deposited in the Mendeley repository (https://data.

Abstract

Di(2-ethylhexyl)phthalate (DEHP) interferes with sex hormones signaling pathways (SHP). C57BL/6J mice prenatally exposed to 300 mg/kg/day DEHP develop a testicular dysgenesis syndrome (TDS) at adulthood, but similarly-exposed FVB/N mice are not affected. Here we aim to understand the reasons behind this drastic difference that should depend on the genome of the strain. In both backgrounds, pregnant female mice received *per os* either DEHP or corn oil vehicle and the male filiations were examined. Computer-assisted sperm analysis showed a DEHP-induced decreased sperm count and velocities in C57BL/6J. Sperm RNA sequencing experiments resulted in the identification of the 62 most differentially expressed RNAs. These RNAs, mainly regulated by hormones, produced strain-specific transcriptional responses to prenatal exposure to DEHP; a pool of RNAs was increased in FVB, another pool of RNAs was decreased in C57BL/6J. In FVB/N, analysis of non-synonymous single nucleotide polymorphisms (SNP) impacting SHP identified rs387782768 and rs29315913 respectively associated with absence of the Forkhead Box A3 (*Foxa3*) RNA and increased expression of estrogen receptor 1 variant 4 (NM_001302533) RNA. Analysis of the role of SNPs modifying SHP binding sites in function of strain-specific responses to DEHP revealed a DEHP-resistance allele in FVB/N containing an additional FOXA1-3 binding site at rs30973633 and four DEHP-induced beta-defensins (*Defb42*, *Defb30*, *Defb47* and *Defb48*). A DEHP-susceptibility allele in C57BL/6J contained five SNPs (rs28279710, rs32977910, rs46648903, rs46677594 and rs48287999) affecting SHP and six genes (*Svs2*, *Svs3b*, *Svs4*, *Svs3a*, *Svs6* and *Svs5)* epigenetically silenced by DEHP. Finally, targeted experiments confirmed increased methylation in the *Svs3ab* promoter with decreased SEMG2 persisting across generations, providing a molecular explanation for the transgenerational sperm velocity decrease found in C57BL/6J after DEHP exposure. We conclude that the existence of SNP-dependent mechanisms in FVB/N inbred mice may confer resistance to transgenerational endocrine disruption.

mendeley.com/datasets/3s94xbbtjx/draft?a=10be535a-1801-4805-977a-1b8d83b058f7).

Funding: This research was supported by the Swiss Centre for Applied Human Toxicology to AG (https://www.scaht.org/) and the Ernst and Lucie Schmidheiny Foundation to LS (http://www.fondation-schmidheiny.ch/).

Competing interests: The authors have declared that no competing interests exist.

Introduction

Di-(2-ethylhexyl) phthalate (DEHP; CAS No. 117-81-7) is a reproductive toxicant and an endocrine disruptor (ED) ubiquitously found in the environment. Accumulated data demonstrate that DEHP interferes with sex steroid hormone signaling pathways (SHP). DEHP and its principal metabolite named mono-(2-ethylhexyl) phthalate (MEHP; CAS No. 4376-20-9) decrease the testosterone produced by testes and interact at the molecular level with the androgen (AR), estrogen (ER) and peroxisome proliferator-activated receptors (PPARs) [1, 2]. Prenatal exposure to DEHP causes androgen deficiency during embryogenesis in both animals and humans [3, 4]. The anogenital distance (AGD), a marker of fetal androgen exposure [5], was shortened in boys born from DEHP-exposed mothers and was reduced in rodents prenatally exposed to DEHP [6–8]. Therefore, the long-term toxicological impacts of prenatal exposure to DEHP are of high concern.

We injected *per os* 300 mg/kg/day DEHP to pregnant mice during embryonic (E) days (E9-19), and measured male fertility parameters at adulthood. The dose was chosen from a previous study and appears to be relevant for extreme human exposure. In fact, the dose of DEHP effectively reaching the mice fetus in the present study was estimated at 190 μg/kg/day and is comparable with the 233 μg/kg/day of median daily intake of DEHP in neonates treated in intensive care units [9]. First, 55% of ingested DEHP is absorbed, whereas DEHP and its derivatives are predominately excreted in the urine. In addition, approximately 20–25% of absorbed DEHP cannot pass the gastrointestinal tract barrier of the pregnant animal or mother, and is excreted in the feces (ToxGuide for DEHP). Thus, a fraction of excreted DEHP is not able to reach the embryos in pregnant females. In fact, only 0.03% of the initial dose of ^{14}C-labelled DEHP, orally administrated to pregnant mice at 8 days of gestation, was recovered in the fetuses when monitoring radioactivity [10]. Among the 9 mg of DEHP that were given per pregnant mice per days, the reconstructed dose of DEHP effectively received by the fetus is estimated at 190 μg/kg/day; 0.27 μg of the initial dose reaches the fetal tissue weighting 1.4 *10–3 kg. That dose is lower than the median daily intake of DEHP calculated in infants in the high-intensiveness product use group. This dose was estimated to range from 233 to 352 μg/kg/day based on MEHHP and MEOHP concentrations recovered in the urines of the preterm infants exposed to DEHP-containing medical products [9]. However, the metabolites that reach the embryos may differ, with DEHP metabolites produced by the exposed mother on one hand, and direct leaching of DEHP from the medical products in the blood circulation of the neonates on the other hand. As a result, a decreased sperm count was observed in the C57BL/6J strain, but not in FVB/N mice, indicating that the latter seem to be resistant and the former sensitive to DEHP [11]. Previously, heterogeneity explained by strains was reported in DEHP-exposed mice [6]. We think that resistance to prenatal exposure to DEHP may imply genetic variations affecting the direct or indirect targets of DEHP, in enzymes responsible for excretion of DEHP, or in DNA sequences recognized by the hormones that are affected by DEHP. The exposure mechanism implies that DEHP orally injected in the mouse mouth cavity passes into the digestive tract of the pregnant female, is metabolized notably in MEHP, enters the blood circulation of pregnant mice, reach the embryos through the cord blood, and exert anti-androgenic and pro-estrogenic activities. The main suspected impact in the male fetus is a decreased production of testosterone. This may trigger long-term impacts on the future sexual health at adulthood, such as in the testicular dysgenesis syndrome (TDS) [12, 13].

The exposure time frame extends from the primordial germ cell (PGC) migration period (~E10.5) and covers the gonadal differentiation period initiated between E11 and E12 in the developing mice embryos, representing a susceptible time window for androgen interference [14]. PGCs are characterized by a specific pattern of DNA methylation and transcription

controlling the cell fate in the lineage [14]. PGCs differentiate themselves in male germ cells during the fetal androgen-dependent sexual differentiation of the somatic gonads to testis. At puberty, a peak of testosterone triggers the spermatogenesis process starting from the spermatogonia. The spermatogenesis involves transcriptional patterns specific to the successive developmental stages [15]. Thus, endocrine disruption taking place during PGCs migration may probably alter DNA methylation and RNA expression status in mature sperm at adulthood.

It has previously been reported that aberrant DNA methylation or dysregulated RNAs in the sperm of adult mice were able to support transgenerational inheritance [16, 17]. Therefore, we studied the transmission of the biological alterations to the subsequent generations taking into account the epigenetic status of genes encoding the dysregulated sperm RNAs. Active transcription is believed to be absent in mature spermatozoa, but RNAs remain present deeply embedded in the sperm nucleus [18]. At least part of these paternal RNAs is transmitted to the egg at fertilization, which may help to understand "unexplained male-factor infertility" [19]. Moreover, a functional AR is expressed in both X and Y carrier spermatozoa and dihydrotestosterone (DHT) is present in the seminal fluid [20]. Additionally, steroid receptors and their ligands may impact on male gamete functions [21].

We postulate that FVB/N resistance or alternatively C57BL/6J susceptibility, may involve genomic variations affecting the androgen signaling occurring in a strain-specific manner. Both DNA methylation and RNA expression may be affected in the sperm of mice prenatally exposed to DEHP, whereas SNP may influence both DNA methylation and gene expression [22]. Comparison between both genomes performed by Wong K. *et al* were incorporated in the present study [23]. Genomes comparison revealed that the AR is not directly affected by polymorphisms in FVB/N compared with the C57BL/6J reference genome. However, the non-synonymous single nucleotide polymorphism (SNP) rs29315913 ("A" in FVB/N and "C" in C57BL/6J) was found in one variant of ESR1 and rs387782768 ("C" in FVB/N and "T" in C57BL/6J) was found in the Forkhead box A3 (FOXA3) transcription factor required for testicular steroidogenesis [23, 24]. Both factors are important for male fertility and are key player of SHP. Briefly, ESR1 is involved in the regulation of male reproductive organs, notably the efferent ductus and the epididymis, and its loss results in impaired ion transport and water reabsorption, with production of abnormal sperm characterized by abnormal flagellar coiling and increased incidence of spontaneous acrosome reactions [25, 26]. The Forkhead box A genes (FOXA1, FOXA2 and FOXA3) encode pioneer transcription factors, i.e. the first detectable factors to engage target sites in chromatin, thus facilitating the further binding of the AR in the nucleus to the targeted recognized DNA sequences [27].

The principal aim of this genome-environment interaction study focalized on male germ cells was to identify SNP varying between FVB/N and C57BL/6J genomes and responsible for the different phenotypes. We postulate that some SNP interacting with DEHP exposure may change the RNA content and the DNA methylation status in the sperm in a strain-specific manner with putative transgenerational inheritance.

Results

Phenotypic impact of *in utero* exposure to DEHP in C57BL/6J and FVB/N mice

The phenotypic changes affecting male fertility parameters induced by prenatal exposure to DEHP confirm the FVB/N resistance found in our earlier study using an independent method [11] and using data partially previously obtained in C57BL/6J [13]. In FVB/N, AGD, testes weight, sperm concentration and curvilinear velocity (VSL) were not affected by prenatal

exposure to DEHP and remain stable also in the second generations of mice generated from the prenatally exposed F1 males (Fig 1A and 1B). The only exception concerns sperm velocities with decreased average path velocity (VAP) and VSL in FVB.D300.F1 compared to FVB.CTL.F1. A return to control values was observed in FVB.D300.F2 (Fig 1B). The experiments were stopped at F2 in FVB/N due to the absence of any remaining impact on all tested parameters.

In contrast, all parameters tested in C57BL/6J were affected by prenatal exposure to DEHP in both the first and second generations in the DEHP-exposed lineage (Fig 1C and 1D). These results are compatible with a DEHP-induced TDS. AGD, sperm concentration and VCL were decreased in C57.D300.F1, and AGD, testes weight, VAP, VCL and VSL were decreased in C57.D300.F2. These multigenerational detrimental impacts of prenatal exposure to DEHP affecting various male fertility parameters are compatible with an intergenerational inheritance in C57BL/6J. Surprisingly, a continuous deterioration of sperm velocity was observed in the DEHP-exposed lineage in the C57BL/6J strain, compatible with a transgenerational increased inheritance of decreased sperm velocity (Fig 1D). At F3 in C57BL/6J, VAP decreased by 24 μm/s between C57.F1.CTL and C57.F3.D300 (p-value = $8.8^{*}10^{-4}$), VCL decreased by 36 μm/s between F1.CTL and F3.D300 (p-value = $3.6^{*}10^{-3}$), and VSL decreased by 24 μm/s between F1.CTL and F3.D300 (p-value = $2.4^{*}10^{-4}$).

Overall, the results demonstrated a strain-specific difference in the impact of prenatal exposure to DEHP in FVB/N compared with C57BL/6J inbred mice. An inbred mice strain is a population of mice clones at the genetic level resulting from a process of at least 20 sequential generations of brother–sister mating. They also strongly suggest the persistence of a detrimental impact across generations in the case of DEHP-susceptibility and revealed a surprising deterioration of sperm velocity apparently inherited in a transgenerational manner (from C57.F1.D300 to C57.F3.D300).

Sperm transcriptome variations induced by prenatal exposure to DEHP in C57BL/6J and FVB/N mice

SHP were shown to be affected by DEHP and its metabolites in previous reports. Both androgens and estrogens exerted their biological effects on gene transcription upon binding to their respective receptors (AR and ESR1). Here, we postulate that prenatal exposure to DEHP may dysregulate sperm RNAs in a persistent manner. Total RNA was extracted from sperm samples analyzed by CASA and the RNA content was analyzed using all-RNA-seq (Fig 2A and S1 Table). One differential analysis was performed using multiple pairwise comparisons between the conditions C57.CTL.F1, C57.D300.F1, FVB.CTL.F1 and FVB.D300.F1 in order to take into account the impact of the strains on sperm RNA content in the absence or presence of DEHP exposure. Additionally, as almost all parameters tested remained affected at F2 in C57BL/6J (Fig 1), we also included the C57.D300.F2 condition.

This approach resulted in genome*environment*generation interactions transcriptomic analysis identifying 62 RNAs as the most differentially expressed RNA among the different conditions (Fig 2B). Importantly, three different patterns of expression changes were found (Fig 2C, 2D and 2E). The first pattern showed increased RNA levels specifically in FVB.D300.F1 compared with FVB.CTL.F1. This pattern presenting an FVB/N-specific and DEHP-mediated induction of RNA expression was associated with FVB/N resistance (Fig 2C). The second pattern was associated with generational changes occurring between the first and second generations in the C57BL/6J exposed lineage (Fig 2D). The third pattern revealed decreased levels of various RNA specifically in C57.D300.F1 compared with C57.CTL.F1, without changes in FVB/N. The latter pattern was associated with C57BL/6J susceptibility to DEHP (Fig 2E). Overall, the 62 differentially expressed RNA across the tested conditions were mainly regulated

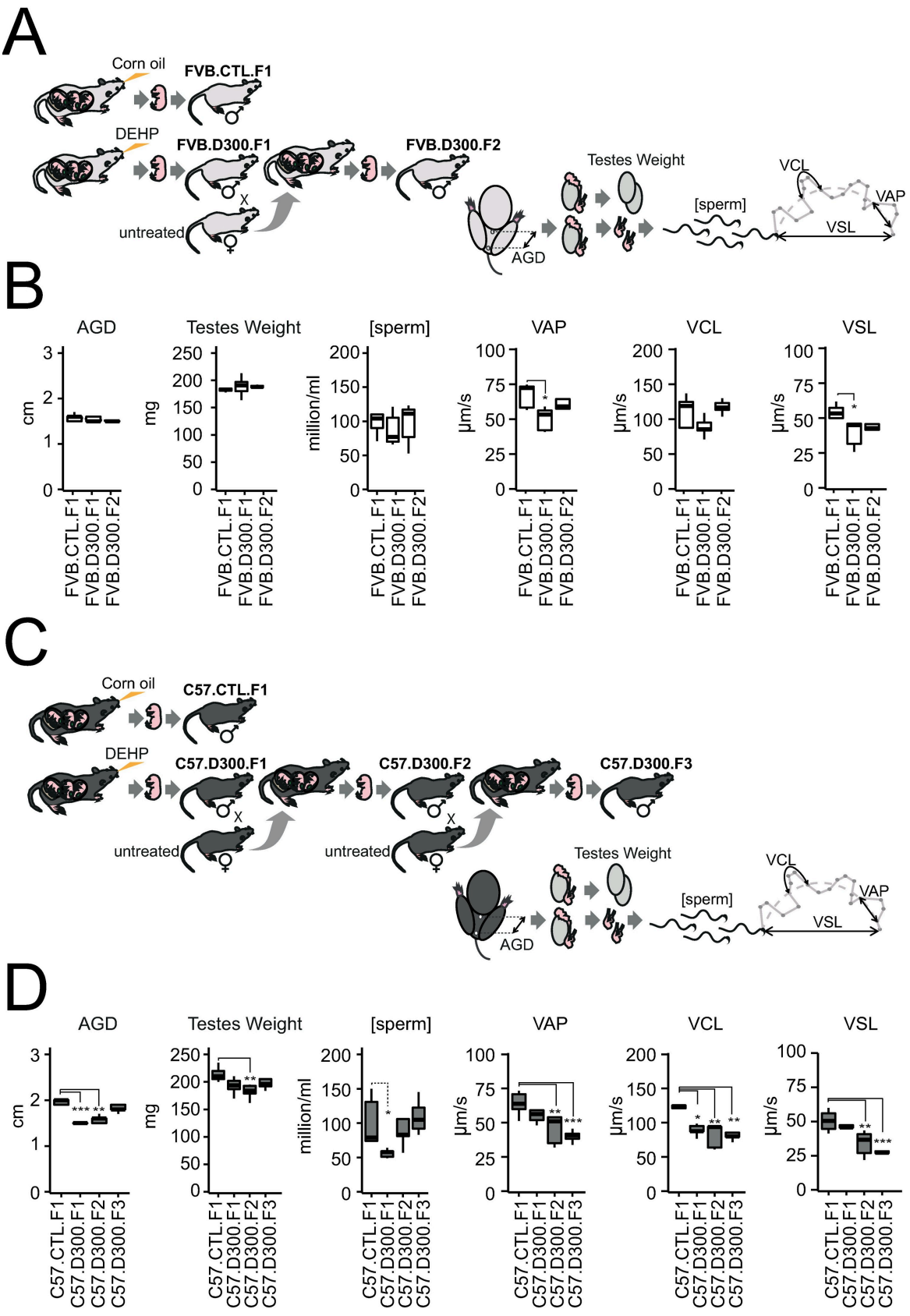
A
Corn oil
FVB.CTL.F1
DEHP
FVB.D300.F1
FVB.D300.F2
X
untreated
Testes Weight
[sperm]
VCL
VAP
VSL
AGD
B
AGD
Testes Weight
[sperm]
VAP
VCL
VSL
cm
mg
million/ml
µm/s
FVB.CTL.F1
FVB.D300.F1
FVB.D300.F2
C
Corn oil
C57.CTL.F1
DEHP
C57.D300.F1
C57.D300.F2
C57.D300.F3
X
untreated
Testes Weight
[sperm]
VCL
VAP
VSL
AGD
D
AGD
Testes Weight
[sperm]
VAP
VCL
VSL
cm
mg
million/ml
µm/s
C57.CTL.F1
C57.D300.F1
C57.D300.F2
C57.D300.F3

Fig 1. Strain-dependent alterations of fertility parameters in male offspring exposed in utero to DEHP. Prenatal exposures to DEHP were performed daily from E9-19 in both FVB/N and C57BL/6J mice strains using per os injections in hand-restrained pregnant females. Injections of 20 μl of 1.15 M DEHP diluted in corn oil corresponding to 300 mg/kg/day (D300) for 30 g mice estimates were compared with injections of 20 μl of corn oil as a vehicle for a fat-soluble compound, settled as the control condition (CTL). Male fertility parameters were obtained at P100 using five biological replicates per condition. AGD and testes weight were obtained prior to computer-assisted sperm analysis (CASA). CASA was used to assess sperm concentrations expressed in million per ml [sperm] and sperm velocities expressed in μm per second (μm/s). VAP: average path velocity; VCL: curvilinear velocity; VSL: straight-line velocity. (A) Experimental design of the study performed in the strain FVB/N. FVB.CTL.F1 were born from the corn oil-exposed mother. FVB.D300.F1 males were born from the DEHP-exposed mother. FVB.D300.F2 males were obtained after mating with unexposed females with FVB.D300.F1. (B). Male fertility parameters obtained in FVB after prenatal exposure to DEHP. AGD, testes weight, sperm concentrations and VCL did not differ across the tested conditions. VAP (p-value <0.02) and VSL (p <0.02) were decreased in FVB.D300.F1 compared with FVB.CTL. F1. (C). Experimental design of the study performed in the strain C57BL/6J. C57.CTL.F1 males were born from the corn oil-exposed mother, whereas C57.D300.F1 males were born from the DEHP-exposed mother. C57.D300.F2 males were obtained after mating with an unexposed female with C57.D300.F1. C57.D300.F3 males were obtained after mating with an unexposed female with C57.D300.F2 males. (D) Male fertility parameters obtained in C57BL/6J strain after prenatal exposure to DEHP. Compared with C57.CTL.F1, AGD, sperm concentration and VCL were decreased in C57.D300.F1 ($p < 7^{*}10^{-5}$, $p < 0.05$, $p < 0.02$, respectively), AGD ($p < 0.002$), testes weight ($p < 0.008$), VAP ($p < 0.008$), VSL ($p < 0.008$) and VCL ($p < 0.003$) were decreased in C57.D300.F2, and VAP ($p < 1^{*}10^{-3}$), VSL ($p < 1^{*}10^{-3}$) and VSL ($p < 0.004$) were decreased in C57.D300.F3. Statistical significance was performed using a one-way analysis of variance with a post-hoc Tukey honestly significant difference test (ANOVA-Tukey HSD). Significant differences between the tested conditions and the control conditions are reported as a graphic. * corrected p-value <0.05, ** corrected p-value <0.01, *** corrected p-values <0.001. Shapiro-Wilk tests reveal that the following parameters most likely followed a normal distribution; weight of the testes ($W = 0.98$, $p = 0.62$), sperm concentration ($W = 0.98$, $p = 0.68$), VAP ($W = 0.97$, $p = 0.39$), VCL ($W = 0.96$, $p = 0.17$) and VSL ($W = 0.96$, $p = 0.17$), whereas AGD ($W = 0.83$, $p = 0.0001$) did not follows a normal distribution. The Bartlett's test for homogeneity of variances reveal equal variance between groups for all parameters; weight of the testes (Bartlett's K-squared = 9.13, df = 6, p = 0.17), AGD (Bartlett's K-squared = 9.18, df = 6, p = 0.16), VAP (Bartlett's K-squared = 4.26, df = 6, p = 0.64); VCL (Bartlett's K-squared = 6, df = 6, p = 0.42), VSL (Bartlett's K-squared = 5.73, df = 6, p = 0.45) and the sperm concentration (Bartlett's K-squared = 12.58, df = 6, p = 0.05). Caution has to be taken in the interpretation of statistical differences in AGD across the tested conditions in the present work due to non-normal distribution of the data.

https://doi.org/10.1371/journal.pone.0208371.g001

by hormones in sperm or in male reproductive tissues (Fig 2F and Table 1). The vast majority (80%) present increased expression during spermatogenesis (Fig 2G); androgen was the most represented regulatory hormone (Fig 2H). In addition, pathways highly relevant to sperm physiological functions and DEHP toxicity were affected *across the tested conditions (S2 Table)*.

Strain-specific non-synonymous SNPs affecting AR, ESR1 and FOXA1-3 sperm RNA levels

SNP variations between FVB/N and C57BL/6J affecting SHP may explain the strain-specificity of the DEHP-induced alterations in sperm RNAs (Fig 2). Non-synonymous SNP rs387782768 in FOXA3 and rs29315913 in ESR1 variant 4 genes were characterized previously [23]. No other relevant SNP affecting SHP could be directly found in both strains. Transcriptomic results of this study revealed that both SNPs were associated with strain-specific differences of particular RNA expression levels, independent of DEHP exposure (Fig 3A). First, rs387782768 was associated with the absence of FOXA3 sperm transcripts in FVB/N. Second, rs29315913 was associated with increased levels of ESR1 variant 4 sperm transcript in FVB/N. Other tested transcription factors not affected by non-synonymous SNP (FOXA1, FOXA2, AR and other ESR1 variants) did not differ in their expression levels between both strains. An upregulation of AR expression was also observed in C57.D300.F2 that did not depend directly on a SNP, apparently reflecting a generational impact in the exposed lineage of the C57BL/6J strain.

These results revealed that strain-specific SNP variations affecting key players in the SHP resulted in differences in sperm RNA levels and they may play a role in the observed strain-specific susceptibility to hormonal disruption.

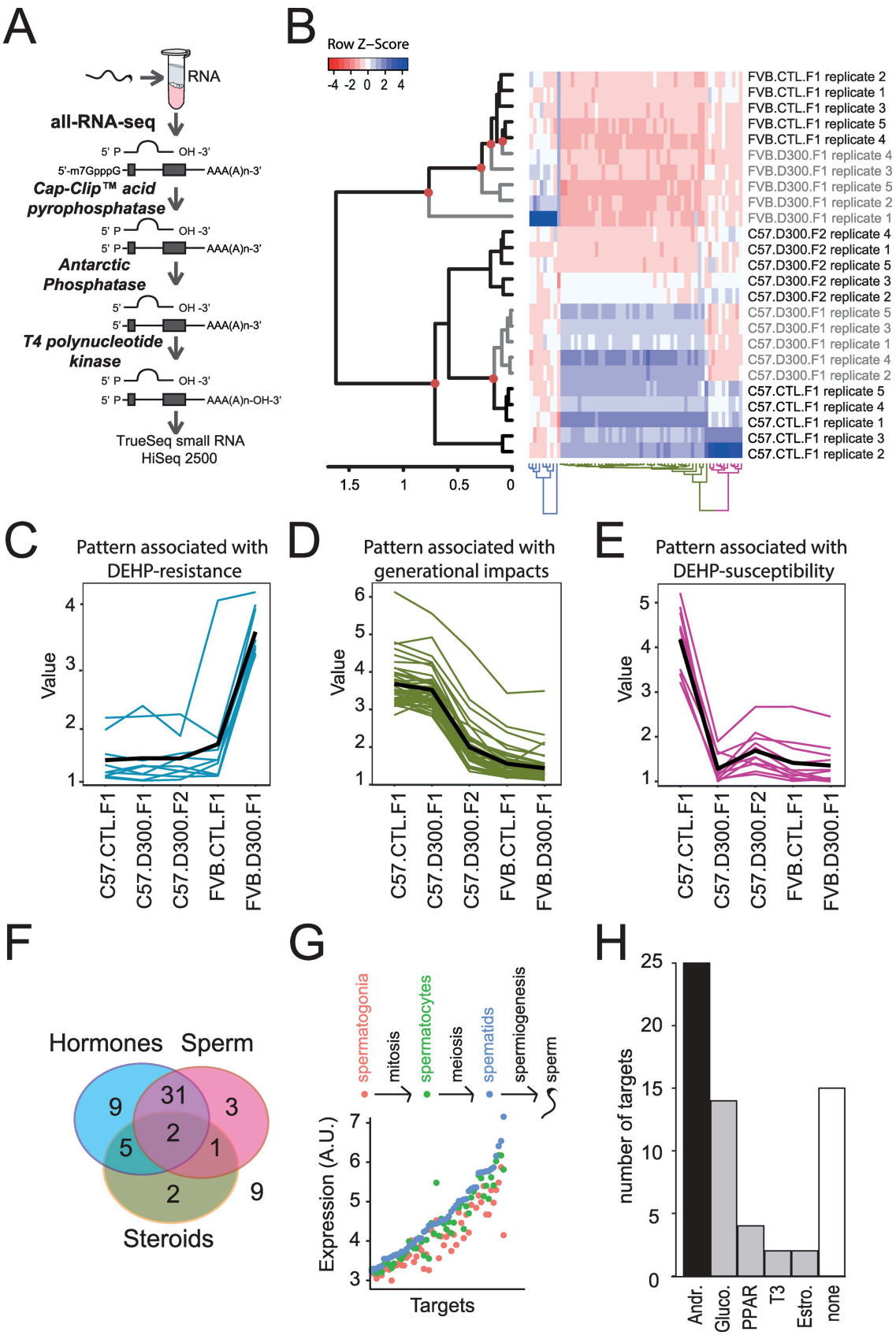
A
RNA
all-RNA-seq
5' P OH -3'
5'-m7GpppG AAA(A)n-3'
Cap-Clip™ acid pyrophosphatase
Antarctic Phosphatase
T4 polynucleotide kinase
AAA(A)n-OH-3'
TrueSeq small RNA
HiSeq 2500
B
Row Z–Score
-4 -2 0 2 4
FVB.CTL.F1 replicate 2
FVB.CTL.F1 replicate 1
FVB.CTL.F1 replicate 3
FVB.CTL.F1 replicate 5
FVB.CTL.F1 replicate 4
FVB.D300.F1 replicate 4
FVB.D300.F1 replicate 3
FVB.D300.F1 replicate 5
FVB.D300.F1 replicate 2
FVB.D300.F1 replicate 1
C57.D300.F2 replicate 4
C57.D300.F2 replicate 1
C57.D300.F2 replicate 5
C57.D300.F2 replicate 3
C57.D300.F2 replicate 2
C57.D300.F1 replicate 5
C57.D300.F1 replicate 3
C57.D300.F1 replicate 1
C57.D300.F1 replicate 4
C57.D300.F1 replicate 2
C57.CTL.F1 replicate 5
C57.CTL.F1 replicate 4
C57.CTL.F1 replicate 1
C57.CTL.F1 replicate 3
C57.CTL.F1 replicate 2
1.5 1 0.5 0
C
Pattern associated with DEHP-resistance
Value
C57.CTL.F1 C57.D300.F1 C57.D300.F2 FVB.CTL.F1 FVB.D300.F1
D
Pattern associated with generational impacts
Value
C57.CTL.F1 C57.D300.F1 C57.D300.F2 FVB.CTL.F1 FVB.D300.F1
E
Pattern associated with DEHP-susceptibility
Value
C57.CTL.F1 C57.D300.F1 C57.D300.F2 FVB.CTL.F1 FVB.D300.F1
F
Hormones Sperm
9 31 3 5 2 1 2 9
Steroids
G
spermatogonia mitosis spermatocytes meiosis spematids spermiogenesis sperm
Expression (A.U.)
Targets
H
number of targets
Andr. Gluco. PPAR T3 Estro. none

Fig 2. Results obtained in the genome*environment*generation transcriptomic interactions study. (A) All-RNA-seq analysis in sperm. Sperm sampled from the cauda epididymis was analyzed in quintuplicates using the all-RNA-seq protocol, which allows measurements of all RNA types independently of their end variations. (B) Hierarchical clustering analysis combined with a heat-map illustration of all-RNA-seq data. Red circles: significant nodes in the dendrogram. In the heat-map, high levels of expression are in blue and low levels in red. (C) The expression pattern associated with the DEHP-resistance indicates induction of expressions in FVB.D300.F1 compared with FVB.CTL.F1. (D) Pattern associated with generational impacts in the C57BL/6J background. Decreased expressions are observed in C57.D300.F2 compared with C57.CTL.F1 and C57.D300.F1. (E) The expression pattern associated with DEHP-susceptibility displayed decreased expressions in C57.D300.F1 compared with C57.CTL.F1. (F) Triple-Venn diagram segregating the 62 RNAs. The 62 RNAs were segregated in a Triple-Venn diagram as hormonally-regulated (light blue circle: N = 47; 76%), as previously identified in sperm (pink circle: N = 37; 60%), or involved in the transport of cholesterol or the metabolism of steroids (yellow circle: N = 10; 16%). The majority of RNAs are hormonally-regulated and expressed in sperm (N = 33; 53%); the minority of RNAs are out of the diagram (N = 9; 15%). (G) Expression levels of RNA across germ cells subtypes: spermatogonia in red, spermatocytes in green, and spermatids in blue. RNAs were significantly enriched for increased expression in spermatogenesis compared with all RNAs in the Chalmel dataset ($\chi^2(1) = 53$; $p < 3.3^{*}10^{-13}$). (H) Number of RNA regulated by androgen (Andr.), glucocorticoids (Gluco.), hormone-like PPARs, triiodothyronine (T3), estrogen (Estro.) or not regulated by hormones (none). 76% of the targets present a reported hormonal regulation (47/62), among these 53% by androgen (25/47).

https://doi.org/10.1371/journal.pone.0208371.g002

Effects of DEHP on promoter methylation and on gene expression in the sperm of both strains

Changes in RNA levels observed in sperm upon prenatal exposure to DEHP may involve alteration in epigenetic mechanisms. Among these, aberrant DNA methylation(s) in the male germ cell lineage caused by prenatal DEHP exposure may result in persistent alterations of sperm RNA patterns detectable at adulthood. To test this hypothesis, all-RNA-seq data were merged to previously acquired Methyl-CpG-binding domain sequencing (MBD-seq) data for all conditions tested at F1 also performed in quintuplicates (C57.CTL.F1, C57.D300.F1, FVB.CTL.F1 and FVB.D300.F1) [11]. The first observation is that transcript abundance was negatively correlated with promoter methylation in the sperm, consistent with a repressive impact of promoter-methylation on transcription named silencing (Fig 3B) [112]. Promoter methylation was then tested specifically in the RNA that produced both patterns associated with either DEHP-susceptibility or DEHP resistance (Fig 2C and 2E and Table 1). The targets for DEHP-susceptibility, characterized by DEHP-induced decreased RNA expression levels, were all associated with a DEHP-induced increased promoter methylation in C57BL/6J (Fig 3B). These combined results are consistent with a DEHP-induced epigenetic silencing of the DEHP-susceptible targets identified only in C57BL/6J, as the same targets were not affected by DEHP in FVB/N, neither in their expression, nor in their promoter methylations levels (Fig 3B). The targets for DEHP-resistance, upregulated by DEHP specifically in FVB/N, were also associated, paradoxically, with promoter methylation increases (Fig 3B). The targets for DEHP-resistance were not affected by DEHP in C57BL/6J, neither in their expressions, nor in their promoter methylation levels (Fig 3B).

We postulated that the decreased expression of androgen-regulated genes in particular may be directly explained by the anti-androgenic activity of DEHP in C57BL/6J, whereas the increased expression of genes in FVB/N may involve an additional pro-estrogenic activity of DEHP. Therefore, the binding sites for both estrogen and androgen signaling systems were analyzed in the promoters of the identified targets for both DEHP-susceptibility and DEHP-resistance (Fig 3C). Results revealed that receptor binding sites for androgen signaling were higher than for estrogen signaling in the promoters of targets for DEHP-susceptibility (Fig 3C), whereas equal numbers of ER and AR binding sites were detected in the promoters of targets for DEHP-resistance (Fig 3C). These results are compatible with anti-androgenic silencing and pro-estrogenic induction of the strain-specific targets.

Overall, these results demonstrate increased promoter methylations in strain-specific affected targets for DEHP-susceptibility in C57BL/6J, and for DEHP-resistance in FVB/N, with differences in the number of ER over AR binding sites found in the promoters of these strain-specific targets.

Table 1. ***Characterization of the 62 dysregulated RNAs.***

Functional Group	Gene Symbol encoding the dysregulated RNA (alternative name)	Associated pattern (Fig 2C, 2D and 2E)	Expression in tissue or cells.	Increased expression in Spermatogenesis: [yes] or [no]. Expression: spermatogonia/ Spermatocytes/ Spermatid. Source data [15].	Protein function	Hormonal-regulation	Ref.
SERPIN & proteases inhibitors	**Serpina1b**	Generational impacts	Spermatozoa	[yes]. 3.89/4.44/4.53	Protease inhibitor	Glucocorticoid	[28, 29]
	Serpina1e	Generational impacts	Spermatozoa	NA/NA/NA	Protease inhibitor	Glucocorticoid	[28, 29]
	Serpina3k	Generational impacts	Spermatozoa	[yes]. 3.28/3.43/3.55	Protease inhibitor	Glucocorticoid	[28, 29]
	Serpinc1	Generational impacts	Spermatozoa	[yes]. 4.17/4.19/4.43	Protease inhibitor	Glucocorticoid	[28, 29]
	Spink1 (Spink3, p12)	DEHP-susceptibility	Spermatozoa	[yes]. 3.37/3.43/3.64	Protease inhibitor	Androgen	[30, 31]
Seminal vesicle secretory proteins	**Sva**	DEHP-susceptibility	Seminal vesicle	[yes]. 3.39/3.54/3.73	Capacitation suppression	Androgen	[32, 33]
	Svs2	DEHP-susceptibility	Seminal vesicle	[yes]. 3.13/3.21/3.36	Semen coagulation (Semenoglin I)	Androgen	[34, 35]
	Svs3a	DEHP-susceptibility	Spermatozoa	[no]. 4.12/4.57/4.53	Semen coagulation (semenogelin II)	Androgen	[36, 37]
	Svs3b	DEHP-susceptibility	Spermatozoa	NA/NA/NA	Semen coagulation (semenogelin II)	Androgen	[36, 37]
	Svs4	DEHP-susceptibility	Spermatozoa	[yes]. 3.26/3.56/4.39	Sperm capacitation inhibitor	Androgen	[36, 38]
	Svs5	DEHP-susceptibility	Seminal vesicle	[no]. 5.30/5.26/5.35	?	Androgen	[39]
	Svs6	DEHP-susceptibility	Seminal vesicle	[yes]. 3.16/3.23/3.30	?	Androgen	[40]
	Pate4 (Svs7)	DEHP-susceptibility	Spermatozoa	[yes]. 3.00/3.31/3.60	Semen liquefaction	Androgen	[41]
Lipocalins	**Lcn5**	DEHP-resistance	Epididymis-specific	[yes]. 4.46/4.96/5.02	Retinoic acid-binding	Androgen	[42–44]
	Lcn8	DEHP-resistance	Epididymis-specific	[yes]. 4.84/5.359/5.364	Retinoic acid-binding	Androgen	[42–44]
	Lcn9	DEHP-resistance	Epididymis-specific	[yes]. 3.75/4.20/4.75	Retinoic acid-binding	Androgen	[42–44]
	Mup3	Generational impacts	Urine	[yes]. 3.34/3.44/3.55	Male-specific pheromone	Androgen	[45]
Defensins	**Defb30**	DEHP-resistance	Epididymis-specific	NA/NA/NA	Innate immune protection	Androgen	[46, 47]
	Spag11b	DEHP-resistance	Epididymis-specific	NA/NA/NA	Innate immune protection	Androgen	[46, 47]
Carboxylesterases	**Ces1c**	Generational impacts	Male reproductive tract	[yes]. 3.47/3.82/3.95	Hydrolysis	Glucocorticoid	[48, 49]
	Ces3a	Generational impacts	Male reproductive tract	NA/NA/NA	Hydrolysis	Androgen	[50] [49, 51]

(*Continued*)

Table 1. (Continued)

Functional Group	Gene Symbol encoding the dysregulated RNA (alternative name)	Associated pattern (Fig 2C, 2D and 2E)	Expression in tissue or cells.	Increased expression in Spermatogenesis: [yes] or [no]. Expression: spermatogonia/ Spermatocytes/ Spermatid. Source data [15].	Protein function	Hormonal-regulation	Ref.
Clotting Factors	**F2**	Generational impacts	Serum & sperm	[yes]. 5.29/5.62/5.83	Blood & seminal clotting	?	[52, 53]
	Fgb	Generational impacts	Serum & sperm	[yes]. 4.07/4.31/5.05	Blood & seminal clotting	Glucocorticoid	[53, 54]
	Plg	Generational impacts	Serum & sperm	[no]. 3.84/4.08/4.05	Blood & seminal clotting	Androgen regulator	[52, 53, 55]
Others	**Gpx5**	DEHP-resistance	Epididymis-specific	[yes]. 3.56/4.13/4.47	oxydative stress protection	Androgen	[56, 57]
	Pon1	Generational impacts	Serum & sperm	[yes]. 4.16/4.47/4.82	removing thiolactone from proteins	Androgen	[58–60]
	Spint4	DEHP-resistance	Epididymis-specific	[yes]. 3.43/3.58/3.66	control Ca2+ uptake by spermatozoa	Androgen	[61, 62]
	9230104L09Rik	DEHP-resistance	Spermatozoa	[yes]. 5.30/6.03/6.16	cysteine protease inhibitor	Androgen	[63]
	Wfdc21	Generational impacts	Epididymis-specific	[yes]. 4.72/4.85/5.02	Innate immune functions	Estrogen	[64–66]
Cholesterol/steroid transport and metabolism	**Apoa1**	Generational impacts	High density lipoprotein & sperm	[yes]. 4.92/5.10/5.32	Cholesterol transport	T3-Thyroid hormone	[67, 68]
	Apoa2	Generational impacts	High density lipoprotein	[yes]. 5.48/6.18/6.41	Cholesterol transport	T3-Thyroid hormone	[69]
	Apoc3	Generational impacts	Very-low-density lipoproteins	[yes]. 3.76/3.98/4.07	Cholesterol transport	H-response enhancer	[70]
	Apoh (beta(2)GPI)	Generational impacts	Liver	[yes]. 4.15/5.81/7.15	Cholesterol transport & placental development and fetal growth	regulated by cis-acting elements	[71]
	Apom	Generational impacts	High density lipoprotein	[yes]. 5.15/5.67/5.73	Cholesterol transport	estrogen	[72]
	Cml2 (Nat8f2)	Generational impacts	Brain and testis	[no]. 3.64/3.99/3.85	Lipids turnover	PPAR	[73]
	Gc (VDB)	Generational impacts	Serum & sperm	[yes]. 3.38/3.65/3.73	Steroid transport (vitamin D)	-	[74, 75]
	Orm1	Generational impacts	Serum & sperm	[yes]. 3.05/3.18/3.30	Steroid transport	Glucocorticoid	[76, 77]
	Cyp2d9	Generational impacts	Liver	[yes]. 3.66/4.03/4.28	Steroid oxidation	Androgen	[78]
	Cyp3a11	Generational impacts	Liver	[no]. 3.22/3.29/3.23	Steroid metabolism	Testosterone hydroxylation	[79]
	Fabp1	Generational impacts	Liver, serum	[yes]. 3.29/3.63/4.23	Fatty acids transport	PPAR	[80]
	Aldob	Generational impacts	Liver	[yes]. 4.67/5.07/5.77	Glycolysis enzyme	Glucocorticoid	[81]
	mir192	Generational impacts	Sperm and adipocytes	NA/NA/NA	Lipid metabolism	Glucocorticoid	[82, 83]
	Saa2	DEHP-susceptibility	Serum & sperm	[yes]. 4.67/4.88/5.07	Cholesterol transport & acute phase	Androgen	[84–86]

(*Continued*)

Table 1. (Continued)

Functional Group	Gene Symbol encoding the dysregulated RNA (alternative name)	Associated pattern (Fig 2C, 2D and 2E)	Expression in tissue or cells.	Increased expression in Spermatogenesis: [yes] or [no]. Expression: spermatogonia/ Spermatocytes/ Spermatid. Source data [15].	Protein function	Hormonal-regulation	Ref.
Glucocorticoid-regulated	**Alb**	Generational impacts	Liver	[yes]. 4.23/4.48/4.63	Hormone carrier	Glucocorticoid	[87]
	Uox	Generational impacts	Liver	[yes]. 3.90/4.89/4.91	Purine catabolism	Glucocorticoid	[88]
	Azgp1	Generational impacts	Adipocyte, prostate	[yes]. 4.97/5.41/5.87	Lipid degradation	Glucocorticoid	[89]
	Cps1	Generational impacts	Testis	[yes]. 4.10/4.30/4.56	Spermatogenesis	Glucocorticoid	[90, 91]
PPARα-dependent	**Slco1b2 (OATP2)**	Generational impacts	Liver	[yes]. 3.27/3.41/3.57	Bile acids uptake	PPAR	[92]
	Sult2a8	Generational impacts	Liver	NA/NA/NA	Conjugation of Dehydroepiandrosterone	PPAR	[93]
Hormones regulators	**Akr1c6 (Hsd17b5)**	Generational impacts	Liver	[no]. 3.39/3.66/3.65	Reduction of androsterone to testosterone	regulator of sex hormones	[94]
	Ahsg (FETUA)	Generational impacts	Serum, bones	[no]. 5.39/5.14/5.75	Mineralization	regulator of lipids hormones	[95]
	Rdh7 (CRAD2)	Generational impacts	Testis	[yes]. 3.58/3.73/3.79	Androgen regulation	regulator of androgens activity	[96, 97]
Probably hormono-dependent	**Hpd**	Generational impacts	Liver	[no]. 4.02/3.87/3.91	Tyrosine catabolism	Hormone	[98]
	Bhmt	Generational impacts	Liver	[no]. 4.53/5.48/4.44	methyltransferase in methionine synthesis	taurine-regulated	[99]
	Hamp	Generational impacts	Hepatocyte and blood	[yes]. 3.61/3.81/4.04	master hormonal regulator of iron	peptide hormone	[100]
	C9	Generational impacts	Serum & sperm	[yes]. 4.21/4.70/5.27	membrane attack complex, antisperm antibody	immuno-regulation	[101–103]
	Slc38a3 (Snat3)	Generational impacts	Brain, Liver, Placenta	[yes]. 5.87/6.17/6.54	transport of amino acids	Glucocorticoid	[104, 105]
Not hormonally regulated	**9530003J23Rik**	DEHP-susceptibility	Spermatozoa	[no]. 3.34/3.23/3.34	?	-	[106]
	Haao	Generational impacts	Brain	[yes]. 4.98/5.59/5.74	synthesis of Quinolinic acid	-	[107]
	Ttc36	Generational impacts	Testis	[yes]. 4.67/5.40/5.77	protein-protein interactions	-	[108]
	Hpx	Generational impacts	Liver	[no]. 4.27/4.46/4.41	serum iron-binding protein	-	[109]
	Rprl3	DEHP-resistance	All cells	NA/NA/NA	tRNA maturation	-	[110]

Overall, these results demonstrate that prenatal exposure to DEHP may alter the male meiotic program in a strain-specific manner, producing distinct patterns of expression changes and mainly implying dysregulation in androgen-regulated sperm RNAs.

https://doi.org/10.1371/journal.pone.0208371.t001

Impact of SNPs on strain-specific DEHP-induced sperm RNA changes

SNP variations affecting binding sites for FOXA1-3, AR and ESR1 and transcription factors were investigated in function of the DEHP-mediated, strain-specific sperm RNA changes (Fig 4). Such an approach may allow the identification of alleles associated with either DEHP-

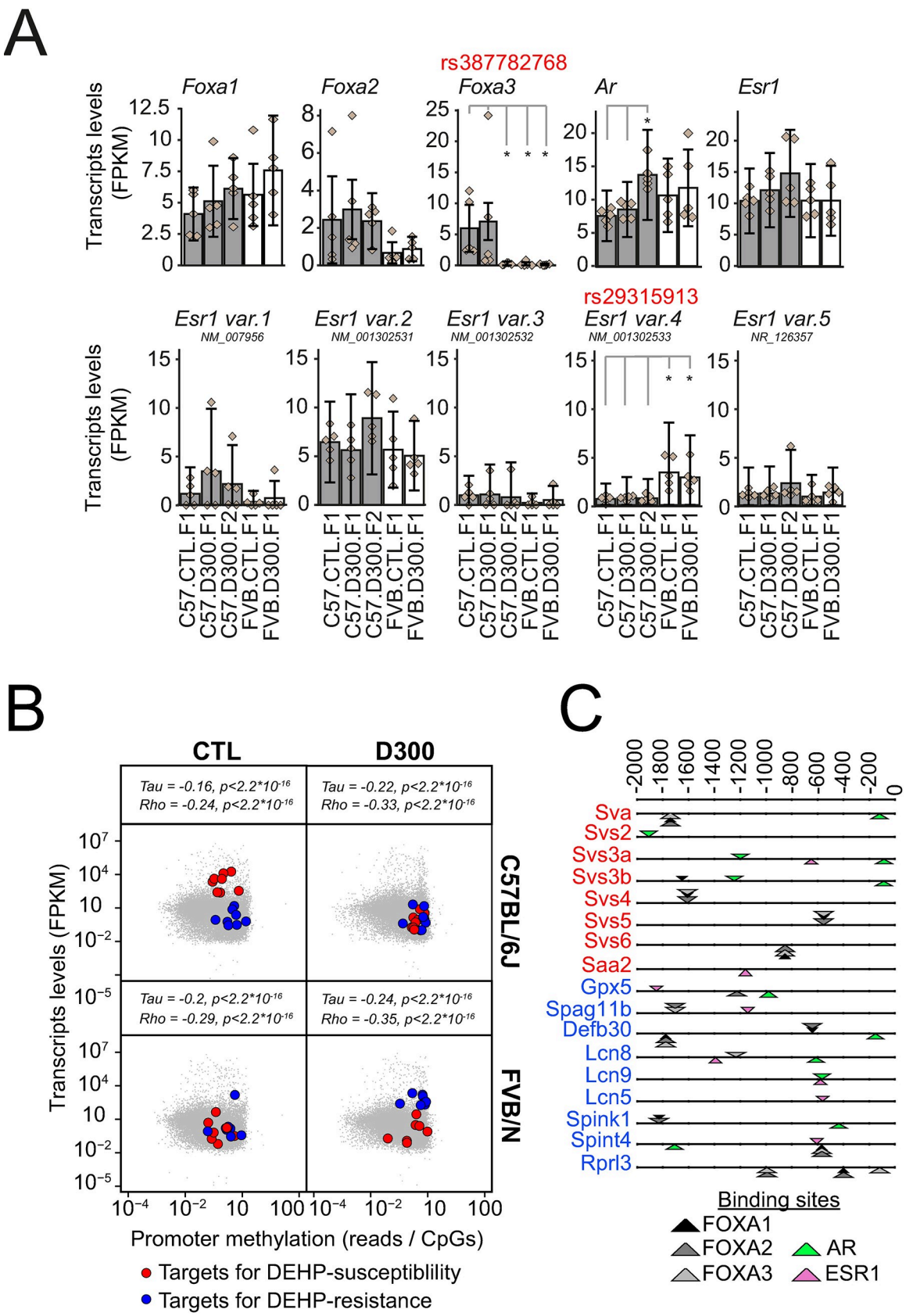
A
rs387782768
Foxa1
Foxa2
Foxa3
Ar
Esr1
Transcripts levels (FPKM)
rs29315913
Esr1 var.1
NM_007956
Esr1 var.2
NM_001302531
Esr1 var.3
NM_001302532
Esr1 var.4
NM_001302533
Esr1 var.5
NR_126357
C57.CTL.F1
C57.D300.F1
C57.D300.F2
FVB.CTL.F1
FVB.D300.F1
B
CTL
D300
Tau = -0.16, p<2.2*10-16
Rho = -0.24, p<2.2*10-16
Tau = -0.22, p<2.2*10-16
Rho = -0.33, p<2.2*10-16
Tau = -0.2, p<2.2*10-16
Rho = -0.29, p<2.2*10-16
Tau = -0.24, p<2.2*10-16
Rho = -0.35, p<2.2*10-16
C57BL/6J
FVB/N
Transcripts levels (FPKM)
Promoter methylation (reads / CpGs)
Targets for DEHP-susceptiblility
Targets for DEHP-resistance
C
Sva
Svs2
Svs3a
Svs3b
Svs4
Svs5
Svs6
Saa2
Gpx5
Spag11b
Defb30
Lcn8
Lcn9
Lcn5
Spink1
Spint4
Rprl3
Binding sites
FOXA1
FOXA2
AR
FOXA3
ESR1

Fig 3. Sexual hormone signaling differs between FVB/N-resistant and C57BL/6J-susceptible strains. (A) Impact of non-synonymous SNP on SHP key players. Expression levels for FOXA1-3 transcription factors, as well as for AR and ESR1, across the five experimental conditions. C57BL/6J-derived data are shown as gray bars and FVB/N derived data as white bars. Error bars represent the CummeRbund computed confidence intervals. Diamonds show the individual FPKM values of the replicates. Data were produced by all RNA-seq. Non-synonymous rs387782768 in FOXA3 and rs29315913 SNP in ESR1 variant 4 were characterized previously [23]. Stars represent statistically significant differences of expression levels according to the non-parametric pairwise Wilcoxon test with Benjamini & Hochberg correction for multiple testing. (B) Promoter methylation and RNA expression in the sperm of the F1 generation of C57BL/6J (up) and FVB/N (down) mice subjected to prenatal exposure to corn oil vehicle (CTL, left) or to DEHP (D300, right) were analyzed in quintuplicates. Promoter methylations were obtained by MBD-seq [11] and were normalized to the number of CpG sites in 2.2 Kb. Correlations were assessed using Kendall's tau and Spearman's rho rank correlation tests. Blue points represent the genes showing the pattern of DEHP-resistance involving Gpx5, Spag11b, Defb30, Lcn8, Lcn9, Lcn5, Spint4 and Rprl3, that was absent in the MBD-seq, but without 9230104L09Rik. Red points represent the genes showing the pattern of DEHP-susceptibility involving Sva, Svs2, Svs3a, Svs3b, Svs4, Svs5, Svs6, Spink1 and Saa2, without Pate4 and 950003J23Rik, both absent in MBD-seq. (C) Binding sites for AR (green), ER (pink) and FOXA1-3 transcription factors (black, dark gray and white) detected in promoters of genes associated with DEHP-susceptibility (red names) and DEHP-resistance (blue names). The number of AR (n = 6) binding sites were higher than ER (n = 2) sites in promoters of genes (n = 8) silenced by DEHP in C57BL/6J and associated with susceptibility. Equal numbers of ER (n = 6) and AR (n = 6) binding sites were detected in the genes (n = 9) induced by DEHP in FVB/N and associated with resistance. Binding sites are shown as triangles orientated differently depending on the DNA strands and with thickness reflecting the score. Sequences were extracted from -2000 to 0 bp with gene names from Mus musculus GRCm38. Analysis was performed using the matrix-scan program of Rsat [111].

https://doi.org/10.1371/journal.pone.0208371.g003

susceptibility or DEHP-resistance if several SNPs are co-localized or if various co-localized genes are affected.

A total of 6 SNPs showed the highest combined impacts on both the strain-specific transcriptional changes induced by prenatal exposure to DEHP measured with Z values, as well as on SHP-motifs specificities measured with δ values (Fig 4A).

We were able to identify rs30973633 as affecting a binding motif for all FOXA1-3 transcription factors in that this motif is present in the FVB/N and absent in the C57BL/6J allele. Moreover, the FVB/N-specific binding motif is associated via a probable DEHP-mediated induction of FOXA1-3 (Fig 3A), with the activation of various beta-defensins localized around rs30973633 (Fig 4B and Table 2). Precisely, prenatal exposure to DEHP induced increased expressions in *Defb42*, *Defb30*, *Defb47* and *Defb48*, but not *Defb43*. None of these genes were affected in their expression after prenatal exposure to DEHP in C57BL/6J (Fig 4B). This DNA region displaying an FVB/N specific induction of RNA expression combined with an FVB/N specific binding site for FOXA1-3 was defined as an "FVB/N resistance allele" to prenatal DEHP exposure.

The second result was the identification of 5 SNP-dependent binding motifs co-localized in the same DNA region encoding the *Svs* genes (Fig 4C). All these SNP-dependent binding motifs were specific to the C57BL/6J allele. More precisely, in the latter, an AR binding site in *Svs4* was affected by two different SNPs (rs28279710 and rs46648903), another AR binding site between *Svs3a* and *Svs6* was affected by rs46677594, an ESR1 binding site upstream of *Svs3b* was affected by rs32977910, and a FOXA2 binding site between *Svs3a* and *Svs6* was affected by rs48287999. All these SNP-dependent binding sites were thus specific of the C57BL/6J allele and all the corresponding genes were silenced by DEHP in C57BL/6J only (Fig 4C and Table 2). This region was defined as the "C57BL/6J susceptibility allele" to prenatal exposure to DEHP.

To summarize, the genome-wide analysis performed resulted in the characterization of the FVB/N resistance allele, involving 4 out of 5 beta-defensins, with all induced by DEHP in FVB/N only, as well as a C57BL/6J susceptibility allele encoding 6 *Svs* genes that were all silenced by DEHP in C57BL/6J only.

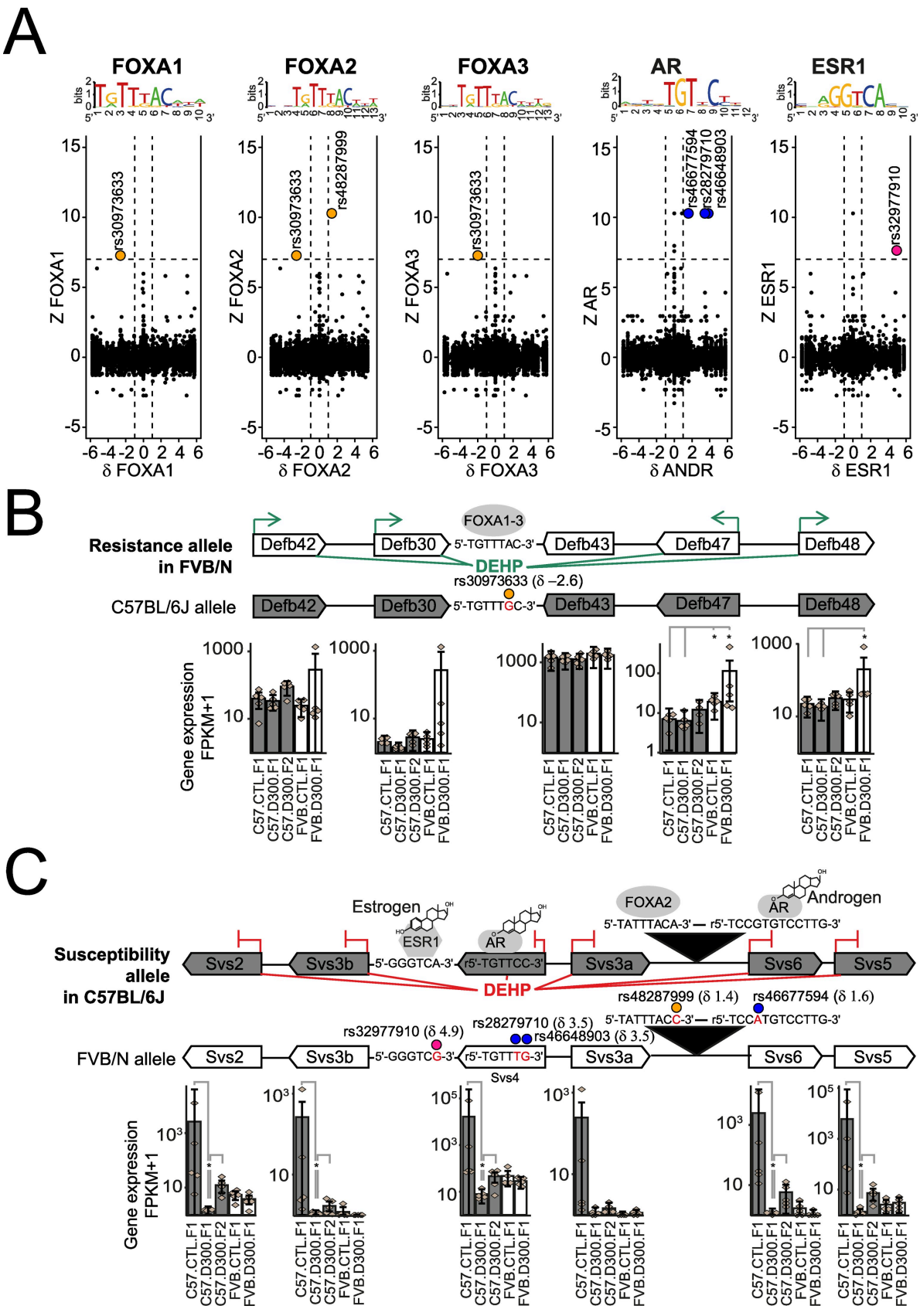
A
FOXA1
FOXA2
FOXA3
AR
ESR1
rs30973633
rs48287999
rs46677594
rs28279710
rs46648903
rs32977910
Z FOXA1
Z FOXA2
Z FOXA3
Z AR
Z ESR1
δ FOXA1
δ FOXA2
δ FOXA3
δ ANDR
δ ESR1
B
Resistance allele in FVB/N
C57BL/6J allele
FOXA1-3
5'-TGTTTAC-3'
DEHP
rs30973633 (δ −2.6)
5'-TGTTTGC-3'
Defb42
Defb30
Defb43
Defb47
Defb48
Gene expression FPKM+1
C57.CTL.F1
C57.D300.F1
C57.D300.F2
FVB.CTL.F1
FVB.D300.F1
C
Susceptibility allele in C57BL/6J
FVB/N allele
Estrogen
Androgen
ESR1
AR
FOXA2
5'-TATTTACA-3' — r5'-TCCGTGTCCTTG-3'
5'-GGGTCA-3'
r5'-TGTTCC-3'
5'-GGGTCG-3'
r5'-TGTTTG-3'
rs48287999 (δ 1.4)
rs46677594 (δ 1.6)
rs28279710 (δ 3.5)
rs46648903 (δ 3.5)
rs32977910 (δ 4.9)
5'-TATTTACC-3' — r5'-TCCATGTCCTTG-3'
Svs2
Svs3b
Svs3a
Svs4
Svs6
Svs5

Fig 4. Genome-wide analysis of SNP impacting SHP motifs in function of strain-specific dysregulation of male germ cell RNAs. (A) Genome-wide analysis of DEHP-induced and strain-specific transcriptional changes (Z) in the function of strain-specific binding site (δ) for FOXA1, FOXA2, FOXA3, AR and ESR1. Z = log2 (FPKM $_{FVB.D300.F1}$ / FPKM $_{FVB.CTL.F1}$)—log2 (FPKM $_{C57.D300.F1}$/ FPKM $_{C57.CTL.F1}$). δ = score $_{C57BL/6J}$ −score $_{FVB/N}$. The corresponding logos above each graph represent the tested motif. Dashed lines represent thresholds. (B) FVB/N-specific DEHP-induced increased expression in the β-defensin loci associated with an FVB/N-specific FOXA1-3 binding motif due to rs30973633. Upon prenatal exposure to DEHP, increased expression levels are recorded for Defb42, Defb30, Defb47 and Defb48, but not for Defb43 in FVB/N, without changes in C57BL/6J. (C) C57BL/6J-specifc DEHP-induced expressional changes in the Svs loci associated with C57BL/6J-specific binding sites for AR, ESR1 and FOXA2 due to SNPs rs28279710, rs46648903, rs46677594, rs32977910 and rs46677594. In utero exposure to DEHP resulted in decreased expression across all Svs genes in C57BL/6J with no change in FVB/N. (BC) Delta values in parentheses represent score differences between both alleles for the respective motif, taking the SNP into account. Stars represent statistically significant differences of expression levels, according to the non-parametric pairwise Wilcoxon test with Benjamini & Hochberg correction for multiple testing. In part C, statistically significant differences between both strains are not shown.

https://doi.org/10.1371/journal.pone.0208371.g004

CpG methylation analysis in C57BL/6J-susceptibility allele combined with quantifications of the semenogelins (SEMG) production in sperm

Two independent targeted methods were applied to validate the previous findings on the susceptibility allele of C57BL/6J (Fig 5A). First, measures of CpG methylation levels were performed using bisulfite pyrosequencing in the promoters of both *Svs2* and *Svs3ab* (Fig 5B). Second, expression levels of SEMG1 and SEMG2 proteins encoded by *Svs2* and *Svs3ab*, respectively, were analyzed by Western blots (Fig 5C and 5E). DNA and protein samples required for these analyzes were extracted by sequential precipitations from the TRIZOL interphase and organic phase that remain in frozen sperm samples after RNA extraction.

The bisulfite pyrosequencing results demonstrated increased methylation levels in three of four CpG sites localized in promoters of both *Svs2 and Svs3ab* in each of the exposed lineages affecting different generations (*Svs2*-CpG_1 methylation increased in C57.D300.F1 and in FVB.D300.F2; *Svs3ab*-CpG_1 methylation increased in both C57.D300.F3 and in FVB.D300.F2; *Svs3ab*-CpG_2 methylation increased in FVB.D300.F2), whereas *Svs2* CpG_2 was always fully methylated (Fig 5B). Methylation levels in both CpG sites of *Svs3ab* promoter were also increased gradually across the exposed lineage in C57BL/6J as revealed by correlations analyses (Fig 5B). Electrophoresis of total protein extracts combined with Western bolt revealed that

Table 2. SNP affecting dysregulated targets by disrupting the binding sites for FOXA1-3, AR and ESR1.

Snp	ref.seq (C57BL/6J)	alt.seq (FVB/NJ)	δ	δ.rev	ref	ref.rev	alt	alt.rev	gene	distance
FOXA1_MOUSE.H11MO.0.A (threshold to p-value: 8.11 for p<0.0001).										
rs30973633	TGTTTGCACA	TGTTTACACA	-2.60	-3.48	7.72	0.00	10.32	3.48	Defb30	10446
FOXA2_MOUSE.H11MO.0.A (threshold to p-value: 8.13 for p<0.0001).										
rs48287999	CACTATTTACAAT	CACTATTTACCAT	1.39	0.00	8.16	0.00	6.76	0.00	Svs4	25871
rs30973633	AGATGTTTGCACA	AGATGTTTACACA	-2.60	-2.22	6.25	0.00	8.86	2.22	Defb30	10446
FOXA3_MOUSE.H11MO.0.A (threshold to p-value: 8.10 for p<0.0001).										
rs30973633	GATGTTTGCACAT	GATGTTTACACAT	-1.99	-1.47	6.73	0.00	8.73	1.47	Defb30	10446
ESR1_MOUSE.H11MO.1.A (threshold to p-value: 7.80 for p<0.0001).										
rs32977910	CTGGGTCACA	CTGGGTCGCA	4.94	0.00	8.37	0.00	3.43	0.00	Svs3b	8536
AR_MOUSE.H11MO.1.A (threshold to p-value: 8.02 for p<0.0001).										
rs28279710	CAGGAACAGGGA	CACGAACAGGGA	0.00	3.50	0	8.41	0	4.907	Svs4	0
rs46648903	CAGGAACAGGGA	CAGAAACAGGGA	0.00	3.59	0	8.41	0	4.825	Svs4	0
rs46677594	CAAGGACACGGA	CAAGGACATGGA	0.00	1.60	0	8.12	0	6.524	Svs4	26567

"Ref": the reference strain C57BL/6J. "Alt": the alternative strain FVB/NJ. "Rev": the reverse strand. The score differences between the alternative and the reference is reported as δ, similarly δ.rev for the reverse strand. Underlined letters in sequences correspond to the SNP in the allele with the lowest δ or δ.rev score. The distance from the nearest gene is in base pairs and the official gene symbol is reported.

https://doi.org/10.1371/journal.pone.0208371.t002

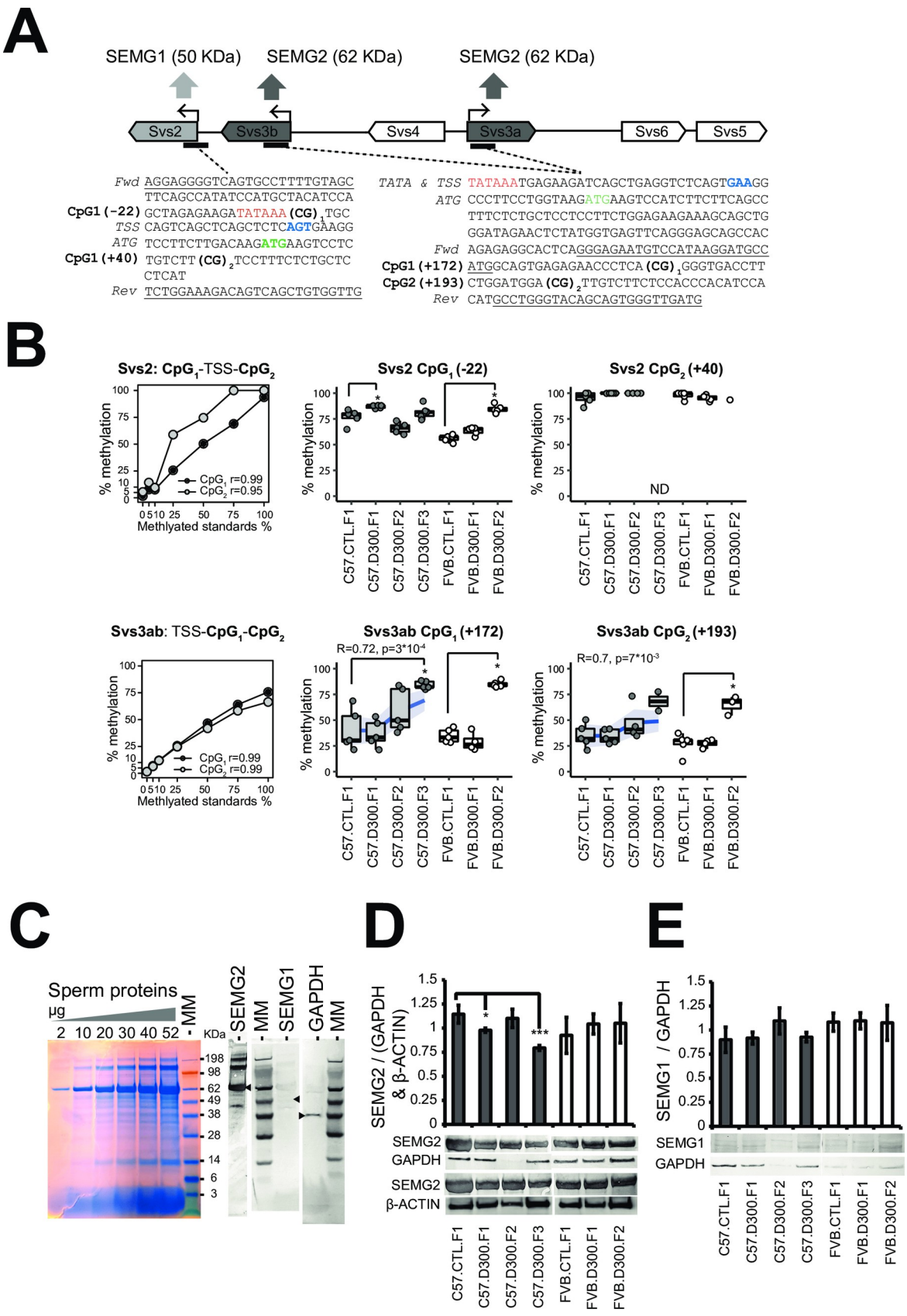
A
SEMG1 (50 KDa)
SEMG2 (62 KDa)
SEMG2 (62 KDa)
Svs2
Svs3b
Svs4
Svs3a
Svs6
Svs5
Fwd AGGAGGGGTCAGTGCCTTTTGTAGC
TTCAGCCATATCCATGCTACATCCA
CpG1 (-22) GCTAGAGAAGATATAAA (CG)1 TGC
TSS CAGTCAGCTCAGCTCTCAGTGAAGG
ATG TCCTTCTTGACAAGATGAAGTCCTC
CpG1 (+40) TGTCTT (CG)2 TCCTTTCTCTGCTC
CTCAT
Rev TCTGGAAAGACAGTCAGCTGTGGTTG
TATA & TSS TATAAATGAGAAGATCAGCTGAGGTCTCAGTGAAGG
ATG CCCTTCCTGGTAAGATGAAGTCCATCTTCTTCAGCC
TTTCTCTGCTCCTCCTTCTGGAGAAGAAAGCAGCTG
GGATAGAACTCTATGGTGAGTTCAGGGAGCAGCCAC
Fwd AGAGAGGCACTCAGGGAGAATGTCCATAAGGATGCC
CpG1 (+172) ATGGCAGTGAGAGAACCCTCA (CG)1 GGGTGACCTT
CpG2 (+193) CTGGATGGA (CG)2 TTGTCTTCTCCACCCACATCCA
Rev CATGCCTGGGTACAGCAGTGGGTTGATG
B
Svs2: CpG1-TSS-CpG2
% methylation
Methlyated standards %
CpG1 r=0.99
CpG2 r=0.95
Svs2 CpG1 (-22)
Svs2 CpG2 (+40)
ND
C57.CTL.F1
C57.D300.F1
C57.D300.F2
C57.D300.F3
FVB.CTL.F1
FVB.D300.F1
FVB.D300.F2
Svs3ab: TSS-CpG1-CpG2
CpG1 r=0.99
CpG2 r=0.99
Svs3ab CpG1 (+172)
R=0.72, p=3*10-4
Svs3ab CpG2 (+193)
R=0.7, p=7*10-3
C
Sperm proteins
µg
2 10 20 30 40 52 - MM
KDa
198
98
62
49
38
28
14
6
3
- SEMG2
- MM
- SEMG1
- GAPDH
- MM
D
SEMG2 / (GAPDH & β-ACTIN)
SEMG2
GAPDH
SEMG2
β-ACTIN
E
SEMG1 / GAPDH
SEMG1
GAPDH

Fig 5. Quantifications of SEMG1-2 combined with measurements of CpG methylation levels in the Svs2 and Svs3ab promoters. (A) Design of bisulfite pyrosequencing assays to measure CpG methylation levels in the promoters of Svs2 encoding SEMG1 and Svs3a/Svs3b encoding SEMG2. Svs3a and Svs3b duplicated-inversed genes are named Svs3ab in part B. The binding sites for the forward and the biotinylated reverse primers used for the bisulfite pyrosequencing experiments are underlined in both original sequences. Two CpG sites were tested in both promoters and numerated CpG_1 and CpG_2. TSS: transcriptional start site as the +1 coordinate's reference in blue. ATG: translational starts in green. TATA: tata boxes in red. (B) CpG methylation levels in both Svs2 and Svs3ab promoters were validated using a pre-mixed calibration standard (0, 5, 10, 25, 50, 75 and 100% Fig 5B and then measured in sperm-extracted DNA under each experimental conditions using bisulfite pyrosequencing in quintuplicates. *Increased methylation levels were found in three of four CpG sites of both promoters in both backgrounds in the DEHP exposed filiations compared with their respective controls; Svs2-CpG_1 in C57.D300.F1 and in FVB.D300.F2 (both $p<10^{-2}$); Svs3ab-CpG_1 in both C57.D300.F3 and in FVB.D300.F2 (both $p<10^{-3}$); Svs3ab-CpG_2 in FVB.D300.F2 ($p<0.04$). Note that methylation levels in the C57BL/6J background correlated positively with the ordered generations in both sites tested in Svs3ab. Each point represents a measure obtained in one mouse. Some measurements did not reach quintuplicates due to full consummation of the DNA samples. (C) Electrophoresis of total sperm protein and Western blots analysis revealed that SEMG2 (62 KDa) is the major protein fraction in sperm. (D) Western blot quantifications revealing decreased SEMG2 in sperm of C57.D300.F1 ($p<0.04$) and C57.D300.F3 ($p<0.004$) compared with C57.CTL.F1. Normalization was performed relative to GAPDH (37 KDa) and β-ACTIN (42 KDa). No changes of SEMG2 were recorded in FVB/N. (E) SEMG1 (50 KDa) levels were low and unchanged across the different conditions tested.

https://doi.org/10.1371/journal.pone.0208371.g005

SEMG2 is the most expressed proteins in sperm samples, whereas SEMG1 was detected at very low levels (Fig 5C). Western blot quantifications revealed decreased SEMG2 specifically in the exposed linage of C57BL/6J at F1 and F3, without changes in FVB/N (Fig 5D). SEMG1 levels were unchanged across the different conditions tested in both backgrounds (Fig 5E).

Overall, the DEHP-induced increased methylation levels recorded at the promoters of *Svs3ab* in the exposed lineage of the strain C57BL/6J were compatible with the observed decreases of SEMG2 expression in C57.D300.F1 and C57.D300.F3 conditions (Fig 5D). In addition, the results provide a molecular explanation for the DEHP-induced transgenerational decrease in sperm velocities recorded in the C57BL/6J lineages (Fig 1D, VAP, VCL and VSL). The latter might be due to the transgenerational inheritance of decreased SEMG2 production mediated by increased promoter methylation in *Svs3ab*. Indeed, it is recognized that a fundamental physiological function of semenogelins is the control of sperm motility [113]. DEHP effects on *Svs3ab* in C57BL/6J strain are coherent with the general consensus, showing an increased methylation, a decreased RNA transcription, and a decreased level of the corresponding protein, SEMG2. DEHP effects on *Svs2* in this same strain are also coherent, showing an increased methylation in the promoter of *Svs2* and a decreased transcription of *Svs2* gene. The absence of effect on the corresponding protein, SEMG1, might be due to technical difficulties associated with the low level of this protein. The results obtained in the FVB/N strain were also coherent with the lack of effect of DEHP, except for the increase in both promoter methylation observed in F2 offspring.

Discussion

C57BL/6J mice prenatally exposed to DEHP present anti-androgenic and pro-estrogenic symptoms, whereas FVB/N mice are phenotypically clearly unaffected (Fig 1). Both SNP affecting directly SHP (rs29315913 and rs387782768) were found to be functional (Fig 3). First, rs29315913 affects the ligand-binding domain of one of the five ESR1 proteins by replacing glycine 447 for a valine due to a C to A conversion in FVB/N [23]. Consequently, NM_001302533 RNA is more expressed in FVB/N. Second, rs387782768 is associated with the absence of FOXA3 in FVB/N (Fig 3A).

FVB/N resistance to DEHP

In FVB/N, a pro-estrogenic impact of DEHP mediated by ESR1 variant 4 (NM_001302533) was detected. NM_001302533 was more expressed in FVB/N containing the SNP-affected

ligand binding domain (Fig 3A) and a 3-fold higher number of ESR1 binding sites was detected across promoters of FVB/N-specific targets (Fig 3C). The involvement of ER in DEHP-mediated toxicity has been reported previously [114]. The pool of targets associated with resistance to DEHP in FVB/N were previously involved in sperm resistance mechanisms (Table 1), against bacterial infections or innate host defense (*Defb30*, *Spag11b*), in protective mechanisms against oxidative stress (*Gpx5*), and in the clearance of exogenous compounds (*Lcn5*, *Lcn9*, *Lcn5*) [44, 115] in accordance with previously reports [116, 117]. We identified a FVB/N-specific binding motif associated with a DEHP-induced induction in loci encoding several β-defensins (Fig 4B). Precisely, rs30973633 was shown to add a FOXA1-3 putative binding motif in the FVB/N allele encoding various beta-defensins overexpressed by DEHP specifically in that strain, with a positive impact of DEHP exposure on FOXA1-3 transcript levels. β-defensins have been shown to play a dual role in the sperm, protecting the sperm from bacterial infections, but also acting in a positive manner on sperm motility [118–124].

C57BL/6J susceptibility to DEHP

In C57BL/6J, the prenatal exposure to DEHP affected all CASA parameters (Fig 1D), reflecting perturbations of SHP such as for the decreased AGD [5], in consistency with meta-analyses [6]. Decreased sperm counts are most probably a consequence of alterations in the proliferation of the fetal male germ cell precursors in the gonadal differentiation period at the time of exposure, or decreased proliferation of Sertoli cells [125]. Decreased testis weight may be due to an alteration in the initial proliferation of all or any gonadal cells lineages or may also involve a long-term pro-estrogenic impact [126]. Interestingly, ER knock-out mice were infertile and showed increased fluid pressure within testes due to the accumulation of the fluid at its production site with decreased sperm counts [127]. Overall, DEHP-mediated anti-androgenic and pro-estrogenic symptoms that remain poorly understood were detected in C57BL/6J, but absent in FVB/N, consistent with an intrinsic resistance of the strain to this recognized endocrine disruptor (Fig 1A and 1B).

In the susceptible C57BL/6J background, initial prenatal exposure to DEHP induced an intergenerational inheritance of anti-androgenic and/or pro-estrogenic symptoms, as well as a transgenerational inheritance of decreased sperm velocity affecting all generations tested up to F3 (Fig 1C and 1D). Importantly, the multigenerational impact found in the C57BL/6J exposed lineage cannot be formally proved in the present study. Indeed, the experimental design lacks F2 and F3 control conditions in both backgrounds, i.e. "FVB.CTL.F2", "C57.CTL.F2" and "C57.CTL.F3". This was due to the priority that was given to perform comparisons between both strains. However, the DEHP-induced transgenerational transmission of decreased sperm velocities recorded in the exposed C57BL/6J seems to be consistent when compared with stable levels recorded for the same parameters in the exposed lineage of the FVB/N strain (Fig 1B and 1D). Previous reports strongly suggest that DEHP may trigger pro-estrogenic and anti-androgenic effects in a multigenerational manner, at least in some strains of mice and rats. Transgenerational inheritance induced by prenatal exposure to DEHP was previously established for cryptorchidism and testicular germ cell in CD-1 outbred mice and Sprague Dawley rats [128, 129], for altered estrous cyclicity and decreased folliculogenesis in female CD-1 mice prenatally exposed to DEHP or to environmentally relevant phthalate mixture [130–133]. Targets for DEHP-susceptibility (Fig 3B and 3C) are the androgen-dependent *Saa2*, the serine peptidase inhibitor Kazal type 1 *Spink1*, the poorly described *9530003J23Rik*, as well as the androgen-dependent *Sva*, *Svs2*, *Svs3a*, *Svs3b*, *Svs4*, *Svs5*, *Svs6* and *Pate4* genes (Table 1). Previous independent reports showed a downregulation of *Svs5* in the fetal testes of Sprague-Dawley outbred CD rats exposed *in utero* to 750 mg/kg per day of DEHP during E12-19 in

association with reduced AGD [134]. Targets were silenced by methylation of their promoters (Fig 3B) that contained AR binding sites, notably in *Sva*, *Svs2* and *Svs3ab* (Fig 3C). In addition, the targets exerted a direct impact on sperm motility (Table 1). The analysis revealed SNPs (rs28279710, rs46648903, rs46677594, rs32977910, rs48287999) affecting sexual hormone-binding sites specific to C57BL/6J and co-localized in the DNA encoding *Svs2*, *Svs3ab*, *Svs4*, *Svs6* and *Svs5* genes. The SNPs may explain the strain-specific DEHP response by rendering the allele more responsive to SHP in C57BL/6J compared with FVB/N (Fig 4C). In C57BL/6J, an apparent DEHP-induced transgenerational inheritance of decreased sperm velocity (Fig 1D) was induced by *in utero* exposure to DEHP and correlates with both silencing of the *Svs3ab* gene (Fig 5B) and the decreased production of SEMG2 (Fig 5D). Among genes encoded by the susceptible allele, *Svs2* encoding SEMG1 and *Svs3ab* encoding SEMG2 are responsible for the production of the two most abundant proteins in sperm known to regulate sperm motility [135].

In conclusion, prenatal exposure to the anti-androgenic DEHP molecule induces intergenerational and transgenerational alterations observed in a susceptible mice background, but not in a resistant mice strain. We found converging evidence for strain-specific, SNP-mediated alterations in androgen-regulated sperm transcripts in association with the alteration of male fertility parameters transmitted across several generations in C57BL/6J. This transmission may be mediated by the epigenetics of the paternal DNA having escaped the erasure-reprogramming system or by other spermatozoa-dependent unknown mechanisms. Biological support for transmission across generations may also involve dysregulated sperm RNA. However, injections of sperm RNA into fertilized oocytes, technically difficult, would be required to formally prove their transmission of the phenotype. We observed that strain-specific genomic variations may confer complex resistance mechanisms. SNPs were identified as associated with the strongest DEHP-induced specific changes in the germ cell content of RNAs coding for proteins required for sperm motility. Finally, the relevance of these findings for humans remains to be investigated. By extrapolation, the results suggest that human embryos exposed to DEHP may not be equally affected in their future reproductive health. According to our findings in mouse, unequal human susceptibility to prenatal exposure to DEHP should first imply genomic variations affecting directly SHP and SNP located in androgen responsive element (ARE). SNP located in ARE, as well as in FOXA1 and ERG binding sites in Human were enriched in prostate cancer susceptibility loci [136], whereas MEHP may advance the progression of prostate cancer through activating the hedgehog pathway [137]. If the purpose is to assess the impact of DEHP on Semenogelin production in human semen, SNP characterized as a quantitative trait loci (eQTL) for SEMG1 and/or SEMG2 should be taken into account. No eQTL are reported for *SEMG2* according to the GTEx portal, whereas 181 eQTL were present in *SEMG1*. Among these eQTL, SNP Rs2233896 introduced a missense in *SEMG1* affecting its expression with a minor allele frequency at 10%, and could therefore represent a good starting candidate. This study shows how mouse genomic variations may be associated with complex resistance mechanisms to prevent the inter- and transgenerational inheritance of altered male fertility parameters. More fundamentally, this study presents a good model to better characterize the array of endocrine signaling and target genes involved in the male reproductive function.

Materials and methods

This study was approved by the Ethics Committee for Animal Experimentation of the University of Geneva Medical School (Geneva, Switzerland) and by the Geneva Cantonal

Veterinarian Office (permit reference: G61/3918) under the licenses GE/9/15 from February 2015 to August 2016 and GE/115/16 since 2017.

All resources used in the present work are given with the Resource Research Identifiers (RRID) number when possible, as recommended by NIH guidelines (https://scicrunch.org/). All the metadata generated in the study were deposited in a publically-available registry for transparency purposes. The data have also been deposited in the NCBI Gene Expression Omnibus [138] as GEO series accession number GSE107839. Files were converted by NCBI to Sequence Read Archive (SRA) files. We reused 10 samples from the previous GEO series accession number GSE86837. The MBD-seq data were reused from the GEO series accession number GSE67159. The analysis of SNPs impacting on hormonal binding motifs in the function of strain-specific RNA responses in male germ cells was deposited in the Mendeley repository (https://data.mendeley.com/datasets/3s94xbbtjx/draft?a=10be535a-1801-4805-977a-1b8d83b058f7).

Experimental mice model

C57BL/6J (Charles River France, RRID:IMSR_JAX:000664) and FVB/N (Charles River Germany, RRID:IMSR_CRL:207) mice were maintained at the animal Core Facility of the University of Geneva Medical School in standard plastic housing cages with *ad libitum* access to food (RM3, SDS Dietex, France) and water, with a 12:12 light cycle. The equipment used at the animal Core Facility of the Geneva Medical School is from Iffa Credo, which became Charles River since 1986. Cages are principally constituted with either polypropylene (example cage "S", ref 081 201) or polycarbonate (example cage "S", ref 081 203). The cover is a stainless steel grid (AISI 304). The bottles are made of rigid polypropylene (example, bottle, ref 088 513) with a stainless steel conical top (example, conical top, ref 088 531). DEHP is never mentioned in the compositions of these products and that material is not suspected to contain DEHP or other phthalates; DEHP is present principally in flexible PVC. However, we cannot exclude traces of DEHP or other phthalates in the animal Core Facility. If DEHP is present in the cages and in the bottles, its level should be very low, otherwise the material would be flexible. Moreover, the levels of DEHP contaminations through the equipment used at the animal Core Facility should be the same across the different experimental conditions, and cannot explain the phenotypical differences observed across these conditions. The ARRIVE checklist for this study is provided (S3 Table).

Prenatal exposure to DEHP and filial generations

One male and one female were mated in the same cage during the night and the presence of a copulatory plug the next day was considered as embryonic day 1 (E1). Prenatal exposure was performed daily from E9-19 covering the sexual differentiation period of the embryos by *per os* injections, using a micro-pipette, of 20 μl fixed volume into the mouth cavity of restrained pregnant female mice. Corn oil delivery vehicle for fat-soluble compounds (Sigma, C8267) was injected in controls (CTL) and 1.15 M DEHP (Fluka-Sigma, DEHP, 80030) diluted in corn oil was injected in exposed mice (D300). The dose of DEHP (CAS No. 117-81-7) was calculated for an estimated mouse weight of 30 g and corresponded to 300 mg of DEHP per kg of mice per day. F1 males prenatally exposed to DEHP were crossed with newly-ordered females of the respective backgrounds to produce F2. The third filial generation (F3) was obtained in the C57BL/6J background only by crossing F2 males with newlyordered females. The experimental design is shown (Fig 1A and 1C).

Computer-assisted sperm analysis and RNA extraction from spermatozoa

Sperm samples were extracted from 100 days of life age-standardized males. The left and right cauda epididymides of each mouse were cleanly dissected and deposited in a petri dish (Falcon, 351008) filled with a pre-warmed 1 ml M2 medium (Sigma, M7167). Epididymides were incised to allow the sperm to swim out during 10 min at 37˚C. Sperm suspensions were transferred in a 100 μm-deep homemade chamber placed on a stage warmer to maintain the temperature at 37˚C during the CASA process (Minitherm, Hamilton Thorme Lac, Beverly, MA, USA). Observations were made with a 4X phase contrast Objective (Olympus, RMS4X) at a final magnification of 40x with fixed parameters. For each sample, a minimum of 400 sperm cells tracks were captured at a rate of 25 images per sec. In parallel, 900 μl of sperm suspension were collected without tissue debris and centrifuge to pellet the sperm. RNA extraction was then performed using TRIZOL according to the manufacturer's recommendations and including glycogen as carrier (Invitrogen, UltraPure Glycogen, Carlsbad, CA, USA). Elution was in 20 μl water (Bioconcept, Water for Molecular Biology DNA/DNAse/RNAse free) and samples were snap-frozen and conserved at -80˚C.

Estimation of the purity of spermatozoa samples

The purity of spermatozoa used to extract RNA was assessed before the procedure by visualizing sperm under a contrast-phase microscope during the CASA process. After RNA sequencing, the purity of sperm RNAs was assessed by read length distributions as corresponding to the profile of mature sperm RNA signatures, involving a peak at 22 for microRNA and a peak at 32 nucleotide for tRNA-derived small RNAs [139]. The read length distribution of all samples is reported (S1 Fig).

Preparation of all-RNA-seq libraries and sequencing

All-RNA-seq was performed as previously described [13]. RNA molecules were treated to be compatible with adapter ligation following a protocol developed by Fasteris SA (Geneva, Switzerland), resulting in RNA molecules carrying a 5'-monophosphate extremity and a free 3'-hydroxyl group independent of their starting differences (Fig 2A). Libraries were prepared using the TruSeq small RNA kit (Illumina Inc., San Diego, CA, USA) and sequenced on a HiSeq 2500 (Illumina Inc.). Base calling was performed using HiSeq Control Software 2.2.58, RTA 1.18.64.0 and CASAVA-1.8.2.

All-RNA-seq reads mapped to mm10 genome and differential quantification

Fastq files were processed on a Linux workstation (Ubuntu 14.04 LTS) and on the "Baobab" high performance computing cluster of the University of Geneva. The analysis was performed using TopHat and Cuffdiff [140]. Quality control of the sequencing process was performed with fastqc ensuring >Q28 in the quality control report for all reads. RA3 adapter sequence was clipped from fastq files and the minimum reads size was settled at 18 pb. Reads were mapped to the mm10 mouse genome using TopHat with appropriate strand-specificity options activated ($ tophat -p 16 -G genes.gtf—library-type fr-secondstrand -o genome reads. fastq). BAM files were indexed and sorted with samtools and reads statistics were computed to summarize the mapping process (S1 Table). Quantifications were performed using TopHat.

Hierarchical cluster analysis and heat map representation

Hierarchical cluster analysis was performed in R with iterative tests involving the diffData function of CummeRbund [141]. A two-dimensional graphical false-color image representation (heatmap) of the gene expression data was produced in R using the heatmap.2 function of the gplots package (Fig 2B) [142].

Analysis of pathways

Selected genes were tested for enrichments using STRING [143, 144]. The analysis was performed online (http://string-db.org/) with the list of official gene symbols and selecting the "*Mus musculus*" organism. The minimum required interaction score was set at the highest confidence level (0.9). A significant enrichment was defined based on a false discovery rate (FDR) <0.01. The representative enrichment per category are reported (S2 Table).

Expression of identified targets in germ cell subtypes

Expression of genes across male germ cell subtypes came from a previously published independent study [15]. Primary spermatocytes and haploid round spermatids were isolated from B6129SF2/J mice at 8–9 weeks, whereas spermatogonia were isolated from testis of 4–8 days postpartum mice using enzymatic digestions of decapsulated testis combined with sedimentation techniques. In our previous study, enriched germ cell populations were analyzed using the microarrays "A-AFFY-45" (Affymetrix GeneChip Mouse Genome 430 2.0). The data were deposited in the ArrayExpress database archived in the European Bioinformatics Institute under the accession number "E-TABM-130". Data were uploaded and integrated in our analysis (Fig 2G).

Combined promoter methylation and RNA expression analysis

All-RNA-seq and MBD-seq data available for all four lineages at F1 were merged by gene symbol in R software separately for both strains (Fig 3B). For each gene, the promoter is defined as the region spanning 2000 bp upstream of the gene's 5'-end to 200 bp downstream. Its methylation level is measured as the number of reads obtained in a 2.2 kilobase probed region divided by the number of CpG in the tested region [11].

Detection of binding sites for the sexual hormone signaling performed in the promoters of the identified targets

Binding sites for FOXA1-3, ESR1 and AR were detected in promoters from -2000 to 0 bp among the selected targets using Rsat [111] (Fig 3B). Briefly, promoter sequences were extracted from *Mus musculus* GRCm38 using a list of official gene names and an analysis was performed using the matrix-scan full option with the same HOCOMOCO position weight matrices (PWM) used afterwards [145].

Genomic variation between FVB/N and C57BL/6J strains

Sequencing and characterization of the FVB/N strain compared with the reference C57BL/6J strain was performed by others [23]. This study generated a catalogue of the major genomic variations specific to FVB/NJ strains corresponding to the FVB/N strain imported into the Jackson Laboratory. When possible, SNPs were verified between both strains analyzed (FVB/N and C57BL/6J) using the all-RNA-seq mapped reads on the IGV and showed concordant genotypes compared with the FVB/NJ and C57BL/6J strains in Wong et al [23] (S2 Fig).

SNP-dependent hormonal binding motifs analyzed in function of strain-specific RNA responses to DEHP exposure

Bioinformatic approaches were used to assess strain-specific SNP affecting binding sites for hormonal controls and genes strain-specifically dysregulated by prenatal exposure to DEHP on genome-wide scale. The R packages and libraries "VariantAnnotation" [146], "Biostrings" [147], "BSgenome.Mmusculus.UCSC.mm10" [148] and "EnsDb.Mmusculus.v79" [149] were required for the analysis. 5'556'605 FVB/NJ SNP variations compared with C57BL/6J were uploaded from the FTP site of the Sanger Institute and filtered to 4'823'906 of high quality. Filtrated SNPs between both strains were used to reconstruct C57BL/6J and FVB/NJ strain-specific alleles with sizes of sequences equal to two times the size of HOCOMOCO position weight matrices (PWM) for mouse AR (named ANDR in the HOCOMOCO PWM and replaced by AR in the present text for simplification purpose), ESR1 and FOXA1-3 [145]. The "matchPWM" function in R was used to computed strain-specific identification scores based on the SNP and the respective scores were reported for the reference (C57BL/6J = ref) and the alternative (FVB/NJ = alt) alleles in both the reverse complement and the positive strand [150]. The results were annotated reporting the distance and the name of the most proximal genes from the SNP-dependent motifs. Genome-wide statistical significances of SNP-dependent detected motifs were based on the HOCOMOCO threshold to p-value relationships. Tables were created with the resulting detected SNP-dependent motifs. Generated tables were then merged individually to the all-RNA-seq derived FPKM data and deposited in Mendeley. SNPs affecting the expression of genes in a strain-specific manner by abolishing or creating a binding motif for FOXA1-3, AR and ESR1 were identified using δ, for motif specificity, in function of Z, reflecting strain-specific transcriptional changes; (delta $<$-1 or $>$ 1, [delta = score (C57BL/6J)–score (FVB/NJ)], Z$<$ -7 or $>$ 7, $[Z = \log2\left(\frac{FPKM+0.1_{FVB.D300.F1}}{FPKM+0.1_{FVB.CTL.F1}}\right) - \log2\left(\frac{FPKM+0.1_{C57.D300.F1}}{FPKM+0.1_{C57.CTL.F1}}\right)]$. The genome-wide significant results are reported (Table 2).

Validation experiments involving bisulfite-pyrosequencing

DNA was extracted using ethanol precipitation from the organic phase of TRIZOL conserved at -20˚C. These samples correspond to the sperm samples obtained during the CASA process that were used for RNA extraction. Bisulfite conversion of DNA was performed using the EZ DNA methylation-Lightning kit (Zymo Research, Irvine, CA, USA; D5030). All assays were validated using methylation standards (EpigenDX, Hopkinton. MA, USA; 80-8060M-PreMix). PCR cycling conditions were 95˚C for 15 min, then 50 cycles of 94˚C for 30 s, 54˚C for 30 s (replaced by 56˚C for 30 s for *Svs3b*), 72˚C for 30 s, with a final elongation during 1 min at 72˚C. Pyrosequencing was performed using a Pyromark Q24 instrument and a workstation from Qiagen (Hilden, Germany) using appropriated enzyme, substrate, nucleotides and reagents. For methylation measured in the *Svs2* promoter, a 175 bp amplicon encompassing 2 CpG sites was generated using forward `5'-AGGAGGGGTTAGTGTTTTTTGTAGT-3'` and biotinylated reverse `5'-[BIO] CAACCACAACTAACTATCTTTCCAAA-3'` primers. The sequencing primer was `5'-GTTATATTTAGTTAGAGAAGATATAAA`. The sequence to analyze was `YGTGTTAGTTAGTTTAGTTTTTAGTGAAGGTTTTTTTTTGATAAGATGAAGTTTTTTGT TTTYGTTTTTTTTTTTGTTTTTTATTTTGGAAAGATAGTTAGTTGTGGTTG` and the dispensation order was `GTCGTGTAGTAGTAGTTAGTGAGTTGACTAGATGAGTTAGTTCTGTTG`. The two CpG sites were validated by methylation standards. For methylation measured in the *Svs3b* gene, a 118 bp amplicon encompassing 2 CpG sites was generated using the forward primer Svs3b_F `5'-GGGAGAATGTTTATAAGGATGTTATG-3'` and the reverse Svs3b_R_biot `5'-[BIO]CATCAACCCACTACTATACCCAAAC3'`. The sequencing primer was the forward

primer. The sequence to analyze was GTAGTGAGAGAATTTTTTAYGGGGTGATTTTTTGGATGGAYGTTGTTTTTTTTATTTATATTTATATGTTTGGGTATAGTAGTGGGTTGATG and the dispensation order was AGCTAGTGAGAGATTGATCGGTGATTGATGTATCGTG. Both CpG sites were validated using methylation standards.

Western blots of SEMG1 and SEMG2

Sperm total protein samples were obtained from TRIZOL fractions after RNA and DNA extractions according to the manufacturer's recommendations by precipitation with 100% isopropanol. Protein pellets were washed with 0.3 M guanidine hydrochloride in 95% ethanol and re-suspended in 200 μl of 0.5% SDS 4 M urea by overnight rotations. Total protein was quantified using the Pierce protein assay 660nm (ThermoFisher Scientific, Waltham, MA, USA; réf. 22662) on a nanodrop ND-100 and using the ionic detergent compatibility reagent (IDCR) (ThermoFisher; réf. 22663). Approximately 20 μg of protein per conditions (C57.CTL.F1, C57.D300.F1, C57.D300.F2, C57.D300.F3, FVB.CTL.F1, FVB.D300.F1 and FVB.D300.F2) were separated on precast Bolt TM 4–12% Bis-Tris gel (ThermoFisher; NW04120) at 150 volts during 45 min and transferred to a nitrocellulose membrane (ThermoFisher, iBlot 2NC Regular Stacks, IB23001) using program P3 on the iBlot2 transfer device (ThermoFisher; IB21001). Membranes were blocked in the SuperBlock (PBS) Blocking Buffer (ThermoFisher; 37515) during 1 h. Five washes of 5 min each were performed between the incubations with Tween-containing TRIS buffer (TBST, ThermoFisher; 28360). Membranes were then incubated 1 h with antibodies diluted in the SuperBlock (PBS) Blocking Buffer. Antibody dilutions were 1:5000 α-SEMG2 polyclonal rabbit anti-mouse [antibodies-online.com, ABIN252161], 1:500 α-SEMG1 polyclonal rabbit anti-mouse [antibodies-online.com, ref ABIN2406262], 1:10,000 α-GAPDH monoclonal rabbit anti-mouse-rat-chicken-human [Abcam, ab181602], before incubation with 1:10,000 secondary antibody goat anti-rabbit IgG alkaline phosphatase secondary (antibodies-online.com, ABIN616373). Revelations were performed with NBT/BCIP Ready-to-Use Tablets (Sigma, c.o. Merck, Darmstadt, Germany, catalogue number: 11697471001). Additionally, membranes were incubated with beta-ACTIN monoclonal antibody coupled to HRP (Sigma, A3854) followed by detection using the ECL Prime Western blot reagents kit (Amersham, Little Chalfont, UK; RPN2232) with images acquired in the myECL Imager with the chemiluminescence mode (ThermoFisher), as an alternative to detect issue with abnormally low levels of GAPDH in condition C57.D300.F2. All images were analyzed using the open source imageJ software.

Statistical analysis

One-way analysis of variance with post-hoc Tukey honestly significant difference test (ANOVA-Tukey HSD) was used to identify means that were significantly different between conditions for the parameters measured with CASA, as well as for AGD and testes weight measurements (Fig 1). The data obtained during the CASA process were tested for following a normal distribution using the Shapiro-Wilk normality test, as well as for homogeneity of the variances across the seven experimental conditions using the Bartlett test of homogeneity of variances. The significance level was set at $p \leq 0.05$. In all-RNA-seq analysis, the CuffDiff computed false-discovery rate adjusted p-values (q-values) were used to identify the transcript levels statistically significantly different between the labeled conditions. Probability estimates for each cluster resulting from the hierarchical cluster analysis were obtained using Pvclust [151]. Pearson's chi-square goodness-of-fit test was computed in R version 3.4.2 using the "chisq.test" function to assess the statistical significance of differences in frequencies of the respective proportions of genes whose expression increases during spermatogenesis among the identified

targets versus all the genes. Correlations between MBD-seq and RNA-seq data were analyzed using non-parametric Kendall's tau and Spearman's rho rank correlations in R (Fig 3B). Non-parametric pairwise Wilcoxon test with Benjamini & Hochberg correction for multiple testing was used to estimate differences of transcript levels between conditions associated with SNPs (Figs 3A and 4) [152]. Parametric Pearson correlations between CpG methylation and the ordered conditions involving C57BL/6J strain were performed in R (Fig 5B).

Supporting information

S1 Fig. Read lengths distribution across samples. A Peaks specific for sperm RNAs were identified. The peak at 22 nucleotides is specific to the size of mature microRNAs. The peak at 32 nucleotides is specific to the size of tRNA-derived small RNAs. The peak at 50 bp involves mainly coding RNAs.
(TIF)

S2 Fig. Example of SNP validation with all RNA-seq reads in a region of interest. Rs28279704 missense mutation validated in the *Svs*4 gene as being "A" in C57BL/6J, reversely in the ATG codon for methionine, and "G" in FVB/N, reversely in the CG codon for threonine.
(TIF)

S1 Table. Read log sheet of all RNA-seq.
(XLSX)

S2 Table. Pathway analysis of the 62 dysregulated RNAs. The statistically significant enrichments in GO terms, KEGG pathways and INTERPRO protein domains identified in the 62 dysregulated sperm RNAs according to the STRING database [144].
(XLSX)

S3 Table. The ARRIVE guidelines checklist for reporting animal data completed for this study.
(DOCX)

Acknowledgments

This research was supported by the Swiss Centre for Applied Human Toxicology and the Ernst and Lucie Schmidheiny Foundation. Computations were performed at the University of Geneva on the Baobab cluster. We are grateful to Yann Sagon for his helpful recommendation to use the Baobab cluster. We are also grateful to Jessica Escoffier and Beatrice Conne for their help. We thank Fasteris SA (Geneva, Switzerland) and NXT-DX (Ghent, Belgium) for the preparation and sequencing of the all RNA-seq and MBD-seq libraries.

Author Contributions

Conceptualization: Ludwig Stenz, Ariane Paoloni-Giacobino.

Data curation: Ludwig Stenz, Julien Prados.

Formal analysis: Ludwig Stenz, Rita Rahban, Julien Prados.

Funding acquisition: Ludwig Stenz, Ariane Paoloni-Giacobino.

Investigation: Ludwig Stenz, Rita Rahban.

Methodology: Ludwig Stenz, Ariane Paoloni-Giacobino.

Project administration: Ludwig Stenz, Rita Rahban, Serge Nef.

Resources: Ludwig Stenz, Serge Nef, Ariane Paoloni-Giacobino.

Software: Ludwig Stenz, Julien Prados.

Supervision: Ariane Paoloni-Giacobino.

Validation: Ludwig Stenz, Julien Prados.

Visualization: Ludwig Stenz.

Writing – original draft: Ludwig Stenz.

Writing – review & editing: Ludwig Stenz, Rita Rahban, Julien Prados, Serge Nef, Ariane Paoloni-Giacobino.

References

1. Engel A, Buhrke T, Imber F, Jessel S, Seidel A, Volkel W, et al. Agonistic and antagonistic effects of phthalates and their urinary metabolites on the steroid hormone receptors ERalpha, ERbeta, and AR. Toxicology letters. 2017; 277:54–63. Epub 2017/06/03. https://doi.org/10.1016/j.toxlet.2017.05.028 PMID: 28571686.
2. Svechnikov K, Svechnikova I, Soder O. Inhibitory effects of mono-ethylhexyl phthalate on steroidogenesis in immature and adult rat Leydig cells in vitro. Reprod Toxicol. 2008; 25(4):485–90. Epub 2008/06/28. https://doi.org/10.1016/j.reprotox.2008.05.057 PMID: 18583092.
3. Borch J, Metzdorff SB, Vinggaard AM, Brokken L, Dalgaard M. Mechanisms underlying the anti-androgenic effects of diethylhexyl phthalate in fetal rat testis. Toxicology. 2006; 223(1–2):144–55. Epub 2006/05/13. https://doi.org/10.1016/j.tox.2006.03.015 PMID: 16690193.
4. Desdoits-Lethimonier C, Albert O, Le Bizec B, Perdu E, Zalko D, Courant F, et al. Human testis steroidogenesis is inhibited by phthalates. Hum Reprod. 2012; 27(5):1451–9. Epub 2012/03/10. https://doi.org/10.1093/humrep/des069 PMID: 22402212.
5. Thankamony A, Pasterski V, Ong KK, Acerini CL, Hughes IA. Anogenital distance as a marker of androgen exposure in humans. Andrology. 2016. Epub 2016/02/06. https://doi.org/10.1111/andr.12156 PMID: 26846869.
6. Dorman DC, Chiu W, Hales BF, Hauser R, Johnson KJ, Mantus E, et al. Systematic reviews and meta-analyses of human and animal evidence of prenatal diethylhexyl phthalate exposure and changes in male anogenital distance. Journal of toxicology and environmental health Part B, Critical reviews. 2018: 1–20. Epub 2018/09/11. https://doi.org/10.1080/10937404.2018.1505354 PMID: 30199328.
7. Swan SH, Main KM, Liu F, Stewart SL, Kruse RL, Calafat AM, et al. Decrease in anogenital distance among male infants with prenatal phthalate exposure. Environmental health perspectives. 2005; 113 (8):1056–61. Epub 2005/08/05. https://doi.org/10.1289/ehp.8100 PMID: 16079079; PubMed Central PMCID: PMC1280349.
8. Latini G, De Felice C, Presta G, Del Vecchio A, Paris I, Ruggieri F, et al. In utero exposure to di-(2-ethylhexyl)phthalate and duration of human pregnancy. Environmental health perspectives. 2003; 111 (14):1783–5. Epub 2003/11/05. https://doi.org/10.1289/ehp.6202 PMID: 14594632; PubMed Central PMCID: PMC1241724.
9. Weuve J, Sanchez BN, Calafat AM, Schettler T, Green RA, Hu H, et al. Exposure to phthalates in neonatal intensive care unit infants: urinary concentrations of monoesters and oxidative metabolites. Environmental health perspectives. 2006; 114(9):1424–31. Epub 2006/09/13. https://doi.org/10.1289/ehp.8926 PMID: 16966100; PubMed Central PMCID: PMC1570064.
10. Tomita I, Nakamura Y, Yagi Y, Tutikawa K. Fetotoxic effects of mono-2-ethylhexyl phthalate (MEHP) in mice. Environmental health perspectives. 1986; 65:249–54. Epub 1986/03/01. https://doi.org/10.1289/ehp.8665249 PMID: 3709449; PubMed Central PMCID: PMC1474685.
11. Prados J, Stenz L, Somm E, Stouder C, Dayer A, Paoloni-Giacobino A. Prenatal Exposure to DEHP Affects Spermatogenesis and Sperm DNA Methylation in a Strain-Dependent Manner. PloS one. 2015; 10(7):e0132136. Epub 2015/08/06. https://doi.org/10.1371/journal.pone.0132136 PMID: 26244509; PubMed Central PMCID: PMC4526524.
12. Virtanen HE, Rajpert-De Meyts E, Main KM, Skakkebaek NE, Toppari J. Testicular dysgenesis syndrome and the development and occurrence of male reproductive disorders. Toxicology and applied

pharmacology. 2005; 207(2 Suppl):501–5. Epub 2005/07/12. https://doi.org/10.1016/j.taap.2005.01.058 PMID: 16005920.

13. Stenz L, Escoffier J, Rahban R, Nef S, Paoloni-Giacobino A. Testicular Dysgenesis Syndrome and Long-Lasting Epigenetic Silencing of Mouse Sperm Genes Involved in the Reproductive System after Prenatal Exposure to DEHP. PloS one. 2017; 12(1):e0170441. Epub 2017/01/14. https://doi.org/10.1371/journal.pone.0170441 PMID: 28085963.

14. Saitou M, Yamaji M. Primordial germ cells in mice. Cold Spring Harbor perspectives in biology. 2012; 4 (11). Epub 2012/11/06. https://doi.org/10.1101/cshperspect.a008375 PMID: 23125014; PubMed Central PMCID: PMC3536339.

15. Chalmel F, Rolland AD, Niederhauser-Wiederkehr C, Chung SS, Demougin P, Gattiker A, et al. The conserved transcriptome in human and rodent male gametogenesis. Proceedings of the National Academy of Sciences of the United States of America. 2007; 104(20):8346–51. Epub 2007/05/08. https://doi.org/10.1073/pnas.0701883104 PMID: 17483452; PubMed Central PMCID: PMC1864911.

16. Gapp K, Jawaid A, Sarkies P, Bohacek J, Pelczar P, Prados J, et al. Implication of sperm RNAs in transgenerational inheritance of the effects of early trauma in mice. Nature neuroscience. 2014; 17 (5):667–9. Epub 2014/04/15. https://doi.org/10.1038/nn.3695 PMID: 24728267; PubMed Central PMCID: PMC4333222.

17. Morgan HD, Sutherland HGE, Martin DIK, Whitelaw E. Epigenetic inheritance at the agouti locus in the mouse. Nature genetics. 1999; 23:314. https://doi.org/10.1038/15490 PMID: 10545949

18. Yan W, Morozumi K, Zhang J, Ro S, Park C, Yanagimachi R. Birth of mice after intracytoplasmic injection of single purified sperm nuclei and detection of messenger RNAs and MicroRNAs in the sperm nuclei. Biology of reproduction. 2008; 78(5):896–902. Epub 2008/02/08. https://doi.org/10.1095/biolreprod.107.067033 PMID: 18256326.

19. Ostermeier GC, Miller D, Huntriss JD, Diamond MP, Krawetz SA. Delivering spermatozoan RNA to the oocyte. Nature. 2004; 429:154. https://doi.org/10.1038/429154a https://www.nature.com/articles/429154a#supplementary-information. PMID: 15141202

20. Zuccarello D, Garolla A, Ferlin A, Menegazzo M, De Toni L, Carraro M, et al. Androgen receptor is expressed in both X- and Y-carrier human spermatozoa. Fertility and sterility. 2009; 91(1):193–200. Epub 2008/03/07. https://doi.org/10.1016/j.fertnstert.2007.11.040 PMID: 18321498.

21. Aquila S, De Amicis F. Steroid receptors and their ligands: effects on male gamete functions. Experimental cell research. 2014; 328(2):303–13. Epub 2014/07/27. https://doi.org/10.1016/j.yexcr.2014.07.015 PMID: 25062984.

22. Dayeh TA, Olsson AH, Volkov P, Almgren P, Ronn T, Ling C. Identification of CpG-SNPs associated with type 2 diabetes and differential DNA methylation in human pancreatic islets. Diabetologia. 2013; 56(5):1036–46. Epub 2013/03/07. https://doi.org/10.1007/s00125-012-2815-7 PMID: 23462794; PubMed Central PMCID: PMC3622750.

23. Wong K, Bumpstead S, Van Der Weyden L, Reinholdt LG, Wilming LG, Adams DJ, et al. Sequencing and characterization of the FVB/NJ mouse genome. Genome Biol. 2012; 13(8):R72. Epub 2012/08/25. https://doi.org/10.1186/gb-2012-13-8-r72 PMID: 22916792; PubMed Central PMCID: PMC3491372.

24. Zhao Y, Li HX, Wang K, Yan BY, Li W. Regulation of testicular steroidogenesis by Foxa3 via transcriptional modulation of ERalpha signaling in type 2 diabetes mellitus (T2DM). Biochemical and biophysical research communications. 2017; 490(3):786–93. Epub 2017/06/25. https://doi.org/10.1016/j.bbrc.2017.06.118 PMID: 28645613.

25. Cooke PS, Nanjappa MK, Ko C, Prins GS, Hess RA. Estrogens in Male Physiology. Physiological reviews. 2017; 97(3):995–1043. Epub 2017/05/26. https://doi.org/10.1152/physrev.00018.2016 PMID: 28539434.

26. Joseph A, Shur BD, Ko C, Chambon P, Hess RA. Epididymal hypo-osmolality induces abnormal sperm morphology and function in the estrogen receptor alpha knockout mouse. Biology of reproduction. 2010; 82(5):958–67. Epub 2010/02/05. https://doi.org/10.1095/biolreprod.109.080366 PMID: 20130266; PubMed Central PMCID: PMC2857636.

27. Kaestner KH. The FoxA factors in organogenesis and differentiation. Current opinion in genetics & development. 2010; 20(5):527–32. Epub 2010/07/02. https://doi.org/10.1016/j.gde.2010.06.005 PMID: 20591647; PubMed Central PMCID: PMC2943037.

28. Dorus S, Wasbrough ER, Busby J, Wilkin EC, Karr TL. Sperm proteomics reveals intensified selection on mouse sperm membrane and acrosome genes. Molecular biology and evolution. 2010; 27 (6):1235–46. Epub 2010/01/19. https://doi.org/10.1093/molbev/msq007 PMID: 20080865; PubMed Central PMCID: PMC2877994.

29. Hammond GL. Plasma steroid-binding proteins: primary gatekeepers of steroid hormone action. The Journal of endocrinology. 2016; 230(1):R13–25. Epub 2016/04/27. https://doi.org/10.1530/JOE-16-0070 PMID: 27113851; PubMed Central PMCID: PMC5064763.

30. Mills JS, Needham M, Parker MG. A secretory protease inhibitor requires androgens for its expression in male sex accessory tissues but is expressed constitutively in pancreas. The EMBO journal. 1987; 6 (12):3711–7. Epub 1987/12/01. PMID: 3428272; PubMed Central PMCID: PMC553841.

31. Zalazar L, Saez Lancellotti TE, Clementi M, Lombardo C, Lamattina L, De Castro R, et al. SPINK3 modulates mouse sperm physiology through the reduction of nitric oxide level independently of its trypsin inhibitory activity. Reproduction. 2012; 143(3):281–95. Epub 2012/01/10. https://doi.org/10.1530/REP-11-0107 PMID: 22228629.

32. Lu SH, Yen YK, Ling TY, Cheng KT, Shu JA, Au HK, et al. Capacitation suppression by mouse seminal vesicle autoantigen involves a decrease in plasma membrane Ca2+-ATPase (PMCA)-mediated intracellular calcium. Journal of cellular biochemistry. 2010; 111(5):1188–98. Epub 2010/08/19. https://doi.org/10.1002/jcb.22844 PMID: 20717922.

33. Yu LC, Chen JL, Tsai WB, Chen YH. Primary structure and characterization of an androgen-stimulated autoantigen purified from mouse seminal-vesicle secretion. The Biochemical journal. 1993; 296 (Pt 3):571–6. Epub 1993/12/15. https://doi.org/10.1042/bj2960571 PMID: 8280054; PubMed Central PMCID: PMC1137736.

34. Araki N, Trencsenyi G, Krasznai ZT, Nizsaloczki E, Sakamoto A, Kawano N, et al. Seminal vesicle secretion 2 acts as a protectant of sperm sterols and prevents ectopic sperm capacitation in mice. Biology of reproduction. 2015; 92(1):8. Epub 2014/11/15. https://doi.org/10.1095/biolreprod.114.120642 PMID: 25395676.

35. Kawano N, Araki N, Yoshida K, Hibino T, Ohnami N, Makino M, et al. Seminal vesicle protein SVS2 is required for sperm survival in the uterus. Proceedings of the National Academy of Sciences of the United States of America. 2014; 111(11):4145–50. Epub 2014/03/05. https://doi.org/10.1073/pnas.1320715111 PMID: 24591616; PubMed Central PMCID: PMC3964112.

36. Araki N, Kawano N, Kang W, Miyado K, Yoshida K, Yoshida M. Seminal vesicle proteins SVS3 and SVS4 facilitate SVS2 effect on sperm capacitation. Reproduction. 2016; 152(4):313–21. Epub 2016/08/04. https://doi.org/10.1530/REP-15-0551 PMID: 27486266.

37. Lin HJ, Luo CW, Chen YH. Localization of the transglutaminase cross-linking site in SVS III, a novel glycoprotein secreted from mouse seminal vesicle. The Journal of biological chemistry. 2002; 277 (5):3632–9. Epub 2001/11/28. https://doi.org/10.1074/jbc.M107578200 PMID: 11723121.

38. Chen YH, Pentecost BT, McLachlan JA, Teng CT. The androgen-dependent mouse seminal vesicle secretory protein IV: characterization and complementary deoxyribonucleic acid cloning. Mol Endocrinol. 1987; 1(10):707–16. Epub 1987/10/01. https://doi.org/10.1210/mend-1-10-707 PMID: 2484712.

39. Simon AM, Veyssiere G, Jean C. Structure and sequence of a mouse gene encoding an androgen-regulated protein: a new member of the seminal vesicle secretory protein family. Journal of molecular endocrinology. 1995; 15(3):305–16. Epub 1995/12/01. PMID: 8748137.

40. Morel L, Brochard D, Manin M, Simon A-M, Jean C, Veyssiere G. Mouse Seminal Vesicle Secretory Protein of 99 Amino Acids (MSVSP99): Characterization and Hormonal and Developmental Regulation. Journal of andrology. 2001; 22(4):549–57. https://doi.org/10.1002/j.1939-4640.2001.tb02214.x PMID: 11451351

41. Luo CW, Lin HJ, Chen YH. A novel heat-labile phospholipid-binding protein, SVS VII, in mouse seminal vesicle as a sperm motility enhancer. The Journal of biological chemistry. 2001; 276(10):6913–21. Epub 2000/12/19. https://doi.org/10.1074/jbc.M006954200 PMID: 11118436.

42. Suzuki K, Yu X, Chaurand P, Araki Y, Lareyre JJ, Caprioli RM, et al. Epididymis-specific lipocalin promoters. Asian journal of andrology. 2007; 9(4):515–21. Epub 2007/06/26. https://doi.org/10.1111/j.1745-7262.2007.00300.x PMID: 17589789.

43. Suzuki K, Yu X, Chaurand P, Araki Y, Lareyre JJ, Caprioli RM, et al. Epididymis-specific promoter-driven gene targeting: a transcription factor which regulates epididymis-specific gene expression. Molecular and cellular endocrinology. 2006; 250(1–2):184–9. Epub 2006/01/18. https://doi.org/10.1016/j.mce.2005.12.043 PMID: 16414179.

44. Suzuki K, Lareyre JJ, Sanchez D, Gutierrez G, Araki Y, Matusik RJ, et al. Molecular evolution of epididymal lipocalin genes localized on mouse chromosome 2. Gene. 2004; 339:49–59. Epub 2004/09/15. https://doi.org/10.1016/j.gene.2004.06.027 PMID: 15363845.

45. Armstrong SD, Robertson DH, Cheetham SA, Hurst JL, Beynon RJ. Structural and functional differences in isoforms of mouse major urinary proteins: a male-specific protein that preferentially binds a male pheromone. The Biochemical journal. 2005; 391(Pt 2):343–50. Epub 2005/06/07. https://doi.org/10.1042/BJ20050404 PMID: 15934926; PubMed Central PMCID: PMC1276933.

46. Hu SG, Zou M, Yao GX, Ma WB, Zhu QL, Li XQ, et al. Androgenic regulation of beta-defensins in the mouse epididymis. Reproductive biology and endocrinology: RB&E. 2014; 12:76. Epub 2014/08/08. https://doi.org/10.1186/1477-7827-12-76 PMID: 25099571; PubMed Central PMCID: PMC4127520.

47. Patil AA, Cai Y, Sang Y, Blecha F, Zhang G. Cross-species analysis of the mammalian beta-defensin gene family: presence of syntenic gene clusters and preferential expression in the male reproductive tract. Physiological genomics. 2005; 23(1):5–17. Epub 2005/07/22. https://doi.org/10.1152/physiolgenomics.00104.2005 PMID: 16033865.

48. von Deimling OH, Wassmer B. Genetic characterization of esterase 28 (ES-28) of the house mouse. Biochemical genetics. 1991; 29(1–2):55–63. Epub 1991/02/01. PMID: 1883319.

49. Zhang Y, Cheng X, Aleksunes L, Klaassen CD. Transcription factor-mediated regulation of carboxylesterase enzymes in livers of mice. Drug metabolism and disposition: the biological fate of chemicals. 2012; 40(6):1191–7. Epub 2012/03/21. https://doi.org/10.1124/dmd.111.043877 PMID: 22429928; PubMed Central PMCID: PMC3362786.

50. Abou-Haila A, Fain-Maurel MA. Selective action of androgens on the molecular forms of esterases characterized by two-dimensional gel electrophoresis in the epididymis and vas deferens of the mouse. International journal of andrology. 1991; 14(3):209–22. Epub 1991/06/01. PMID: 2066165.

51. Mikhailov AT, Torrado M. Carboxylesterases moonlight in the male reproductive tract: a functional shift pivotal for male fertility. Frontiers in bioscience: a journal and virtual library. 2000; 5:E53–62. Epub 2000/07/06. PMID: 10877995.

52. Lwaleed B, Jackson C, Greenfield R, Stewart A, Delves G, Birch B, et al. Seminal tissue factor revisited. International journal of andrology. 2006; 29(2):360–7. Epub 2005/12/24. https://doi.org/10.1111/j.1365-2605.2005.00608.x PMID: 16371111.

53. Lwaleed BA, Greenfield R, Stewart A, Birch B, Cooper AJ. Seminal clotting and fibrinolytic balance: a possible physiological role in the male reproductive system. Thrombosis and haemostasis. 2004; 92(4):752–66. Epub 2004/10/07. https://doi.org/10.1160/TH04-03-0142 PMID: 15467906.

54. Amrani DL. Regulation of fibrinogen biosynthesis: glucocorticoid and interleukin-6 control. Blood coagulation & fibrinolysis: an international journal in haemostasis and thrombosis. 1990; 1(4–5):443–6. Epub 1990/10/01. PMID: 2133221.

55. Okaji Y, Tashiro Y, Gritli I, Nishida C, Sato A, Ueno Y, et al. Plasminogen deficiency attenuates postnatal erythropoiesis in male C57BL/6 mice through decreased activity of the LH-testosterone axis. Experimental hematology. 2012; 40(2):143–54. Epub 2011/11/08. https://doi.org/10.1016/j.exphem.2011.10.008 PMID: 22056679.

56. Lareyre JJ, Claessens F, Rombauts W, Dufaure JP, Drevet JR. Characterization of an androgen response element within the promoter of the epididymis-specific murine glutathione peroxidase 5 gene. Molecular and cellular endocrinology. 1997; 129(1):33–46. Epub 1997/04/25. PMID: 9175627.

57. Perry AC, Jones R, Niang LS, Jackson RM, Hall L. Genetic evidence for an androgen-regulated epididymal secretory glutathione peroxidase whose transcript does not contain a selenocysteine codon. The Biochemical journal. 1992; 285 (Pt 3):863–70. Epub 1992/08/01. https://doi.org/10.1042/bj2850863 PMID: 1386734; PubMed Central PMCID: PMC1132876.

58. Aitken RJ, Flanagan HM, Connaughton H, Whiting S, Hedges A, Baker MA. Involvement of homocysteine, homocysteine thiolactone, and paraoxonase type 1 (PON-1) in the etiology of defective human sperm function. Andrology. 2016; 4(2):345–60. Epub 2016/01/31. https://doi.org/10.1111/andr.12157 PMID: 26825875.

59. Cheng X, Klaassen CD. Hormonal and chemical regulation of paraoxonases in mice. The Journal of pharmacology and experimental therapeutics. 2012; 342(3):688–95. Epub 2012/06/02. https://doi.org/10.1124/jpet.112.194803 PMID: 22653878; PubMed Central PMCID: PMC3422525.

60. Tavilani H, Fattahi A, Esfahani M, Khodadadi I, Karimi J, Bahrayni E, et al. Genotype and phenotype frequencies of paraoxonase 1 in fertile and infertile men. Systems biology in reproductive medicine. 2014; 60(6):361–6. Epub 2014/09/30. https://doi.org/10.3109/19396368.2014.960624 PMID: 25264968.

61. Chen LY, Lin YH, Lai ML, Chen YH. Developmental profile of a caltrin-like protease inhibitor, P12, in mouse seminal vesicle and characterization of its binding sites on sperm surface. Biology of reproduction. 1998; 59(6):1498–505. Epub 1998/11/26. https://doi.org/10.1095/biolreprod59.6.1498 PMID: 9828198.

62. Penttinen J, Pujianto DA, Sipila P, Huhtaniemi I, Poutanen M. Discovery in silico and characterization in vitro of novel genes exclusively expressed in the mouse epididymis. Mol Endocrinol. 2003; 17(11):2138–51. Epub 2003/08/16. https://doi.org/10.1210/me.2003-0008 PMID: 12920233.

63. Li Y, Friel PJ, McLean DJ, Griswold MD. Cystatin E1 and E2, new members of male reproductive tract subgroup within cystatin type 2 family. Biology of reproduction. 2003; 69(2):489–500. Epub 2003/04/18. https://doi.org/10.1095/biolreprod.102.014100 PMID: 12700194.

64. Bingle CD, Vyakarnam A. Novel innate immune functions of the whey acidic protein family. Trends in immunology. 2008; 29(9):444–53. Epub 2008/08/05. https://doi.org/10.1016/j.it.2008.07.001 PMID: 18676177.

65. Chen Y, Wang S, Liu T, Wu Y, Li JL, Li M. WAP four-disulfide core domain protein 2 gene(WFDC2) is a target of estrogen in ovarian cancer cells. Journal of ovarian research. 2016; 9:10. Epub 2016/03/02. https://doi.org/10.1186/s13048-015-0210-y PMID: 26928556; PubMed Central PMCID: PMC4770698.

66. Clauss A, Lilja H, Lundwall A. A locus on human chromosome 20 contains several genes expressing protease inhibitor domains with homology to whey acidic protein. The Biochemical journal. 2002; 368 (Pt 1):233–42. Epub 2002/11/06. https://doi.org/10.1042/BJ20020869 PMID: 12206714; PubMed Central PMCID: PMC1222987.

67. Agarwal A, Sharma R, Durairajanayagam D, Ayaz A, Cui Z, Willard B, et al. Major protein alterations in spermatozoa from infertile men with unilateral varicocele. Reproductive biology and endocrinology: RB&E. 2015; 13:8. Epub 2015/04/19. https://doi.org/10.1186/s12958-015-0007-2 PMID: 25890347; PubMed Central PMCID: PMC4383193.

68. Romney JS, Chan J, Carr FE, Mooradian AD, Wong NC. Identification of the thyroid hormone-responsive messenger RNA spot 11 as apolipoprotein-A1 messenger RNA and effects of the hormone on the promoter. Mol Endocrinol. 1992; 6(6):943–50. Epub 1992/06/01. https://doi.org/10.1210/mend.6.6.1495493 PMID: 1495493.

69. Strobl W, Chan L, Patsch W. Differential regulation of hepatic apolipoprotein A-I and A-II gene expression by thyroid hormone in rat liver. Atherosclerosis. 1992; 97(2–3):161–70. Epub 1992/12/01. PMID: 1466661.

70. Kardassis D, Tzameli I, Hadzopoulou-Cladaras M, Talianidis I, Zannis V. Distal apolipoprotein C-III regulatory elements F to J act as a general modular enhancer for proximal promoters that contain hormone response elements. Synergism between hepatic nuclear factor-4 molecules bound to the proximal promoter and distal enhancer sites. Arteriosclerosis, thrombosis, and vascular biology. 1997; 17 (1):222–32. Epub 1997/01/01. PMID: 9012660.

71. Robertson SA, Roberts CT, van Beijering E, Pensa K, Sheng Y, Shi T, et al. Effect of beta2-glycoprotein I null mutation on reproductive outcome and antiphospholipid antibody-mediated pregnancy pathology in mice. Molecular human reproduction. 2004; 10(6):409–16. Epub 2004/04/22. https://doi.org/10.1093/molehr/gah058 PMID: 15100383.

72. Wei J, Yu Y, Luo GH, Feng YH, Shi YP, Zhang J, et al. 17beta-estradiol regulates the expression of apolipoprotein M through estrogen receptor alpha-specific binding motif in its promoter. Lipids in health and disease. 2017; 16(1):66. Epub 2017/04/01. https://doi.org/10.1186/s12944-017-0458-x PMID: 28359281; PubMed Central PMCID: PMC5374570.

73. Pessentheiner AR, Pelzmann HJ, Walenta E, Schweiger M, Groschner LN, Graier WF, et al. NAT8L (N-acetyltransferase 8-like) accelerates lipid turnover and increases energy expenditure in brown adipocytes. The Journal of biological chemistry. 2013; 288(50):36040–51. Epub 2013/10/25. https://doi.org/10.1074/jbc.M113.491324 PMID: 24155240; PubMed Central PMCID: PMC3861652.

74. Lerchbaum E, Obermayer-Pietsch B. Vitamin D and fertility: a systematic review. European journal of endocrinology / European Federation of Endocrine Societies. 2012; 166(5):765–78. Epub 2012/01/26. https://doi.org/10.1530/EJE-11-0984 PMID: 22275473.

75. Potsch-Schneider L, Klein H. Subtyping of group specific component (GC) in human semen, blood and vaginal fluid by isoelectric focusing in immobilized pH gradients. Electrophoresis. 1988; 9(9):602–5. Epub 1988/09/01. https://doi.org/10.1002/elps.1150090923 PMID: 3243258.

76. Fournier T, Medjoubi NN, Porquet D. Alpha-1-acid glycoprotein. Biochimica et biophysica acta. 2000; 1482(1–2):157–71. Epub 2000/11/04. PMID: 11058758.

77. Panidis D, Rousso D, Panidou E, Asseo P. Orosomucoid levels in the seminal plasma or fertile and infertile men. Archives of andrology. 1993; 30(3):161–4. Epub 1993/05/01. PMID: 8498868.

78. Dkhil MA, Al-Quraishy S, Abdel-Baki AA, Ghanjati F, Arauzo-Bravo MJ, Delic D, et al. Epigenetic modifications of gene promoter DNA in the liver of adult female mice masculinized by testosterone. The Journal of steroid biochemistry and molecular biology. 2015; 145:121–30. Epub 2014/12/03. https://doi.org/10.1016/j.jsbmb.2014.11.006 PMID: 25448745.

79. Shi R, Wu J, Meng C, Ma B, Wang T, Li Y, et al. Cyp3a11-mediated testosterone-6beta-hydroxylation decreased, while UGT1a9-mediated propofol O-glucuronidation increased, in mice with diabetes mellitus. Biopharmaceutics & drug disposition. 2016; 37(7):433–43. Epub 2016/08/16. https://doi.org/10.1002/bdd.2027 PMID: 27514509.

80. Schachtrup C, Emmler T, Bleck B, Sandqvist A, Spener F. Functional analysis of peroxisome-proliferator-responsive element motifs in genes of fatty acid-binding proteins. The Biochemical journal.

2004; 382(Pt 1):239–45. Epub 2004/05/08. https://doi.org/10.1042/BJ20031340 PMID: 15130092; PubMed Central PMCID: PMC1133936.

81. Ito J, Kuzumaki T, Otsu K, Iuchi Y, Ishikawa K. Hormonal regulation of aldolase B gene expression in rat primary cultured hepatocytes. Archives of biochemistry and biophysics. 1998; 350(2):291–7. Epub 1998/03/21. PMID: 9473304.

82. Krattinger R, Bostrom A, Schioth HB, Thasler WE, Mwinyi J, Kullak-Ublick GA. microRNA-192 suppresses the expression of the farnesoid X receptor. American journal of physiology Gastrointestinal and liver physiology. 2016; 310(11):G1044–51. Epub 2016/04/16. https://doi.org/10.1152/ajpgi.00297.2015 PMID: 27079614.

83. Short AK, Fennell KA, Perreau VM, Fox A, O'Bryan MK, Kim JH, et al. Elevated paternal glucocorticoid exposure alters the small noncoding RNA profile in sperm and modifies anxiety and depressive phenotypes in the offspring. Translational psychiatry. 2016; 6(6):e837. Epub 2016/06/15. https://doi.org/10.1038/tp.2016.109 PMID: 27300263; PubMed Central PMCID: PMC4931607.

84. Delic D, Ellinger-Ziegelbauer H, Vohr HW, Dkhil M, Al-Quraishy S, Wunderlich F. Testosterone response of hepatic gene expression in female mice having acquired testosterone-unresponsive immunity to Plasmodium chabaudi malaria. Steroids. 2011; 76(10–11):1204–12. Epub 2011/06/15. https://doi.org/10.1016/j.steroids.2011.05.013 PMID: 21669218.

85. Timur H, Kokanali MK, Inal HA, Tuzluoglu D, Yilmaz N. A study on the association between serum amyloid A and sperm concentration. Andrologia. 2016; 48(6):626–30. Epub 2015/10/07. https://doi.org/10.1111/and.12491 PMID: 26437740.

86. Tomita T, Ieguchi K, Sawamura T, Maru Y. Human serum amyloid A3 (SAA3) protein, expressed as a fusion protein with SAA2, binds the oxidized low density lipoprotein receptor. PloS one. 2015; 10(3):e0118835. Epub 2015/03/05. https://doi.org/10.1371/journal.pone.0118835 PMID: 25738827; PubMed Central PMCID: PMC4349446.

87. Moshage HJ, de Haard HJ, Princen HM, Yap SH. The influence of glucocorticoid on albumin synthesis and its messenger RNA in rat in vivo and in hepatocyte suspension culture. Biochimica et biophysica acta. 1985; 824(1):27–33. Epub 1985/01/29. PMID: 3967027.

88. Raab LS, Decker GL, Jonas AJ, Kaetzel MA, Dedman JR. Glucocorticoid regulation of rat liver urate oxidase. Journal of cellular biochemistry. 1991; 47(1):18–30. Epub 1991/09/01. https://doi.org/10.1002/jcb.240470104 PMID: 1939364.

89. Russell ST, Tisdale MJ. The role of glucocorticoids in the induction of zinc-alpha2-glycoprotein expression in adipose tissue in cancer cachexia. British journal of cancer. 2005; 92(5):876–81. Epub 2005/02/17. https://doi.org/10.1038/sj.bjc.6602404 PMID: 15714206; PubMed Central PMCID: PMC2361908.

90. Huo R, Zhu H, Lu L, Ying L, Xu M, Xu Z, et al. Molecular cloning, identification and characteristics of a novel isoform of carbamyl phosphate synthetase I in human testis. Journal of biochemistry and molecular biology. 2005; 38(1):28–33. Epub 2005/02/18. PMID: 15715943.

91. Lamers WH, Vink C, Charles R. Role of thyroid hormones in the normal and glucocorticosteroid hormone-induced evolution of carbamoyl-phosphate synthase (ammonia) activity in axolotl liver. Comparative biochemistry and physiology B, Comparative biochemistry. 1978; 59(2):103–10. Epub 1978/01/01. PMID: 318276.

92. Cheng X, Klaassen CD. Critical role of PPAR-alpha in perfluorooctanoic acid- and perfluorodecanoic acid-induced downregulation of Oatp uptake transporters in mouse livers. Toxicological sciences: an official journal of the Society of Toxicology. 2008; 106(1):37–45. Epub 2008/08/16. https://doi.org/10.1093/toxsci/kfn161 PMID: 18703564; PubMed Central PMCID: PMC2563139.

93. Feng L, Yuen YL, Xu J, Liu X, Chan MY, Wang K, et al. Identification and characterization of a novel PPARalpha-regulated and 7alpha-hydroxyl bile acid-preferring cytosolic sulfotransferase mL-STL (Sult2a8). Journal of lipid research. 2017; 58(6):1114–31. Epub 2017/04/27. https://doi.org/10.1194/jlr.M074302 PMID: 28442498; PubMed Central PMCID: PMC5454508.

94. Rheault P, Charbonneau A, Luu-The V. Structure and activity of the murine type 5 17beta-hydroxysteroid dehydrogenase gene(1). Biochimica et biophysica acta. 1999; 1447(1):17–24. Epub 1999/09/29. PMID: 10500239.

95. Brylka L, Jahnen-Dechent W. The role of fetuin-A in physiological and pathological mineralization. Calcified tissue international. 2013; 93(4):355–64. Epub 2013/01/02. https://doi.org/10.1007/s00223-012-9690-6 PMID: 23277412.

96. Su J, Chai X, Kahn B, Napoli JL. cDNA cloning, tissue distribution, and substrate characteristics of a cis-Retinol/3alpha-hydroxysterol short-chain dehydrogenase isozyme. The Journal of biological chemistry. 1998; 273(28):17910–6. Epub 1998/07/04. https://doi.org/10.1074/jbc.273.28.17910 PMID: 9651397.

97. Tomita K, Sato M, Kajiwara K, Tanaka M, Tamiya G, Makino S, et al. Gene structure and promoter for Crad2 encoding mouse cis-retinol/3alpha-hydroxysterol short-chain dehydrogenase isozyme. Gene. 2000; 251(2):175–86. Epub 2000/07/06. PMID: 10876094.

98. Awata H, Endo F, Matsuda I. Structure of the human 4-hydroxyphenylpyruvic acid dioxygenase gene (HPD). Genomics. 1994; 23(3):534–9. Epub 1994/10/01. https://doi.org/10.1006/geno.1994.1540 PMID: 7851880.

99. Jurkowska H, Niewiadomski J, Hirschberger LL, Roman HB, Mazor KM, Liu X, et al. Downregulation of hepatic betaine:homocysteine methyltransferase (BHMT) expression in taurine-deficient mice is reversed by taurine supplementation in vivo. Amino acids. 2016; 48(3):665–76. Epub 2015/10/21. https://doi.org/10.1007/s00726-015-2108-9 PubMed Central PMCID: PMC4924537. PMID: 26481005

100. Nemeth E, Ganz T. Regulation of iron metabolism by hepcidin. Annual review of nutrition. 2006; 26:323–42. Epub 2006/07/20. https://doi.org/10.1146/annurev.nutr.26.061505.111303 PMID: 16848710

101. Bozas SE, Kirszbaum L, Sparrow RL, Walker ID. Several vascular complement inhibitors are present on human sperm. Biology of reproduction. 1993; 48(3):503–11. Epub 1993/03/01. https://doi.org/10.1095/biolreprod48.3.503 PMID: 7680906

102. D'Cruz OJ, Haas GG Jr., Wang BL, DeBault LE. Activation of human complement by IgG antisperm antibody and the demonstration of C3 and C5b-9-mediated immune injury to human sperm. J Immunol. 1991; 146(2):611–20. Epub 1991/01/25. PMID: 1987279

103. Kirszbaum L, Sharpe JA, Murphy B, d'Apice AJ, Classon B, Hudson P, et al. Molecular cloning and characterization of the novel, human complement-associated protein, SP-40,40: a link between the complement and reproductive systems. The EMBO journal. 1989; 8(3):711–8. Epub 1989/03/01. PMID: 2721499; PubMed Central PMCID: PMC400866.

104. Karinch AM, Lin CM, Meng Q, Pan M, Souba WW. Glucocorticoids have a role in renal cortical expression of the SNAT3 glutamine transporter during chronic metabolic acidosis. American journal of physiology Renal physiology. 2007; 292(1):F448–55. Epub 2006/09/07. https://doi.org/10.1152/ajprenal.00168.2006 PMID: 16954343.

105. Rubio-Aliaga I, Wagner CA. Regulation and function of the SLC38A3/SNAT3 glutamine transporter. Channels (Austin). 2016; 10(6):440–52. Epub 2016/07/01. https://doi.org/10.1080/19336950.2016.1207024 PMID: 27362266; PubMed Central PMCID: PMC5034772.

106. Dean MD, Clark NL, Findlay GD, Karn RC, Yi X, Swanson WJ, et al. Proteomics and comparative genomic investigations reveal heterogeneity in evolutionary rate of male reproductive proteins in mice (Mus domesticus). Molecular biology and evolution. 2009; 26(8):1733–43. Epub 2009/05/08. https://doi.org/10.1093/molbev/msp094 PMID: 19420050; PubMed Central PMCID: PMC2734151.

107. Calderone V, Trabucco M, Menin V, Negro A, Zanotti G. Cloning of human 3-hydroxyanthranilic acid dioxygenase in Escherichia coli: characterisation of the purified enzyme and its in vitro inhibition by Zn2+. Biochimica et biophysica acta. 2002; 1596(2):283–92. Epub 2002/05/15. PMID: 12007609.

108. Zhou Y, He Q, Chen J, Liu Y, Mao Z, Lyu Z, et al. The expression patterns of Tetratricopeptide repeat domain 36 (Ttc36). Gene expression patterns: GEP. 2016; 22(2):37–45. Epub 2016/11/09. https://doi.org/10.1016/j.gep.2016.11.001 PMID: 27826126.

109. Bu JT, Bartnikas TB. The use of hypotransferrinemic mice in studies of iron biology. Biometals: an international journal on the role of metal ions in biology, biochemistry, and medicine. 2015; 28(3):473–80. Epub 2015/02/11. https://doi.org/10.1007/s10534-015-9833-0 PMID: 25663418; PubMed Central PMCID: PMC4430341.

110. Li K, Williams RS. Cloning and characterization of three new murine genes encoding short homologues of RNase P RNA. The Journal of biological chemistry. 1995; 270(42):25281–5. Epub 1995/10/20. https://doi.org/10.1074/jbc.270.42.25281 PMID: 7559668.

111. Turatsinze JV, Thomas-Chollier M, Defrance M, van Helden J. Using RSAT to scan genome sequences for transcription factor binding sites and cis-regulatory modules. Nature protocols. 2008; 3(10):1578–88. Epub 2008/09/20. https://doi.org/10.1038/nprot.2008.97 PMID: 18802439.

112. Newell-Price J, Clark AJ, King P. DNA methylation and silencing of gene expression. Trends in endocrinology and metabolism: TEM. 2000; 11(4):142–8. Epub 2001/02/07. PMID: 10754536.

113. de Lamirande E. Semenogelin, the main protein of the human semen coagulum, regulates sperm function. Seminars in thrombosis and hemostasis. 2007; 33(1):60–8. Epub 2007/01/27. https://doi.org/10.1055/s-2006-958463 PMID: 17253191.

114. Kawano M, Qin XY, Yoshida M, Fukuda T, Nansai H, Hayashi Y, et al. Peroxisome proliferator-activated receptor alpha mediates di-(2-ethylhexyl) phthalate transgenerational repression of ovarian Esr1 expression in female mice. Toxicology letters. 2014; 228(3):235–40. Epub 2014/05/09. https://doi.org/10.1016/j.toxlet.2014.04.019 PMID: 24811840.

115. Flower DR. The lipocalin protein family: structure and function. The Biochemical journal. 1996; 318 (Pt 1):1–14. Epub 1996/08/15. https://doi.org/10.1042/bj3180001 PMID: 8761444; PubMed Central PMCID: PMC1217580.

116. Suna S, Yamaguchi F, Kimura S, Tokuda M, Jitsunari F. Preventive effect of D-psicose, one of rare ketohexoses, on di-(2-ethylhexyl) phthalate (DEHP)-induced testicular injury in rat. Toxicology letters. 2007; 173(2):107–17. Epub 2007/08/19. https://doi.org/10.1016/j.toxlet.2007.06.015 PMID: 17698303.

117. Gaido KW, Hensley JB, Liu D, Wallace DG, Borghoff S, Johnson KJ, et al. Fetal mouse phthalate exposure shows that Gonocyte multinucleation is not associated with decreased testicular testosterone. Toxicological sciences: an official journal of the Society of Toxicology. 2007; 97(2):491–503. Epub 2007/03/16. https://doi.org/10.1093/toxsci/kfm049 PMID: 17361019.

118. Zhang C, Zhou Y, Xie S, Yin Q, Tang C, Ni Z, et al. CRISPR/Cas9-mediated genome editing reveals the synergistic effects of beta-defensin family members on sperm maturation in rat epididymis. FASEB journal: official publication of the Federation of American Societies for Experimental Biology. 2018; 32 (3):1354–63. Epub 2017/11/17. https://doi.org/10.1096/fj.201700936R PMID: 29141997.

119. Yu H, Dong J, Gu Y, Liu H, Xin A, Shi H, et al. The novel human beta-defensin 114 regulates lipopolysaccharide (LPS)-mediated inflammation and protects sperm from motility loss. The Journal of biological chemistry. 2013; 288(17):12270–82. Epub 2013/03/14. https://doi.org/10.1074/jbc.M112.411884 PMID: 23482568; PubMed Central PMCID: PMC3636911.

120. Zhao Y, Diao H, Ni Z, Hu S, Yu H, Zhang Y. The epididymis-specific antimicrobial peptide beta-defensin 15 is required for sperm motility and male fertility in the rat (Rattus norvegicus). Cellular and molecular life sciences: CMLS. 2011; 68(4):697–708. Epub 2010/08/10. https://doi.org/10.1007/s00018-010-0478-4 PMID: 20694738.

121. Fernandez-Fuertes B, Narciandi F, O'Farrelly C, Kelly AK, Fair S, Meade KG, et al. Cauda Epididymis-Specific Beta-Defensin 126 Promotes Sperm Motility but Not Fertilizing Ability in Cattle. Biology of reproduction. 2016; 95(6):122. Epub 2016/10/21. https://doi.org/10.1095/biolreprod.116.138792 PMID: 27707713; PubMed Central PMCID: PMC5333942.

122. Cao D, Li Y, Yang R, Wang Y, Zhou Y, Diao H, et al. Lipopolysaccharide-induced epididymitis disrupts epididymal beta-defensin expression and inhibits sperm motility in rats. Biology of reproduction. 2010; 83(6):1064–70. Epub 2010/09/10. https://doi.org/10.1095/biolreprod.109.082180 PMID: 20826730.

123. Diao R, Fok KL, Chen H, Yu MK, Duan Y, Chung CM, et al. Deficient human beta-defensin 1 underlies male infertility associated with poor sperm motility and genital tract infection. Science translational medicine. 2014; 6(249):249ra108. Epub 2014/08/15. https://doi.org/10.1126/scitranslmed.3009071 PMID: 25122636.

124. Zhou CX, Zhang Y-L, Xiao L, Zheng M, Leung KM, Chan MY, et al. An epididymis-specific β-defensin is important for the initiation of sperm maturation. Nature Cell Biology. 2004; 6:458. https://doi.org/10.1038/ncb1127 PMID: 15122269

125. Rebourcet D, Darbey A, Monteiro A, Soffientini U, Tsai YT, Handel I, et al. Sertoli Cell Number Defines and Predicts Germ and Leydig Cell Population Sizes in the Adult Mouse Testis. Endocrinology. 2017; 158(9):2955–69. Epub 2017/09/16. https://doi.org/10.1210/en.2017-00196 PMID: 28911170; PubMed Central PMCID: PMC5659676.

126. Sharpe RM. Do males rely on female hormones? Nature. 1997; 390:447. https://doi.org/10.1038/37236 PMID: 9393994

127. Hess RA. Oestrogen in fluid transport in efferent ducts of the male reproductive tract. Reviews of reproduction. 2000; 5(2):84–92. Epub 2000/06/24. PMID: 10864852.

128. Doyle TJ, Bowman JL, Windell VL, McLean DJ, Kim KH. Transgenerational effects of di-(2-ethylhexyl) phthalate on testicular germ cell associations and spermatogonial stem cells in mice. Biology of reproduction. 2013; 88(5):112. Epub 2013/03/29. https://doi.org/10.1095/biolreprod.112.106104 PMID: 23536373; PubMed Central PMCID: PMC4013901.

129. Chen J, Wu S, Wen S, Shen L, Peng J, Yan C, et al. The Mechanism of Environmental Endocrine Disruptors (DEHP) Induces Epigenetic Transgenerational Inheritance of Cryptorchidism. PloS one. 2015; 10(6):e0126403. Epub 2015/06/04. https://doi.org/10.1371/journal.pone.0126403 PMID: 26035430; PubMed Central PMCID: PMC4452760.

130. Zhou C, Gao L, Flaws JA. Exposure to an Environmentally Relevant Phthalate Mixture Causes Transgenerational Effects on Female Reproduction in Mice. Endocrinology. 2017; 158(6):1739–54. Epub 2017/04/04. https://doi.org/10.1210/en.2017-00100 PMID: 28368545; PubMed Central PMCID: PMC5460945.

131. Brehm E, Rattan S, Gao L, Flaws JA. Prenatal Exposure to Di(2-Ethylhexyl) Phthalate Causes Long-Term Transgenerational Effects on Female Reproduction in Mice. Endocrinology. 2018; 159(2):795–809. Epub 2017/12/12. https://doi.org/10.1210/en.2017-03004 PMID: 29228129.

132. Rattan S, Brehm E, Gao L, Niermann S, Flaws JA. Prenatal exposure to di(2-ethylhexyl) phthalate disrupts ovarian function in a transgenerational manner in female mice. Biology of reproduction. 2018; 98 (1):130–45. Epub 2017/11/23. https://doi.org/10.1093/biolre/iox154 PMID: 29165555; PubMed Central PMCID: PMC5803793.

133. Pocar P, Fiandanese N, Berrini A, Secchi C, Borromeo V. Maternal exposure to di(2-ethylhexyl)phthalate (DEHP) promotes the transgenerational inheritance of adult-onset reproductive dysfunctions through the female germline in mice. Toxicology and applied pharmacology. 2017; 322:113–21. Epub 2017/03/14. https://doi.org/10.1016/j.taap.2017.03.008 PMID: 28286118.

134. Liu K, Lehmann KP, Sar M, Young SS, Gaido KW. Gene expression profiling following in utero exposure to phthalate esters reveals new gene targets in the etiology of testicular dysgenesis. Biology of reproduction. 2005; 73(1):180–92. Epub 2005/02/25. https://doi.org/10.1095/biolreprod.104.039404 PMID: 15728792.

135. Mitra A, Richardson RT, O'Rand MG. Analysis of recombinant human semenogelin as an inhibitor of human sperm motility. Biology of reproduction. 2010; 82(3):489–96. Epub 2009/11/06. https://doi.org/10.1095/biolreprod.109.081331 PMID: 19889947; PubMed Central PMCID: PMC2825168.

136. Dadaev T, Saunders EJ, Newcombe PJ, Anokian E, Leongamornlert DA, Brook MN, et al. Fine-mapping of prostate cancer susceptibility loci in a large meta-analysis identifies candidate causal variants. Nature communications. 2018; 9(1):2256. Epub 2018/06/13. https://doi.org/10.1038/s41467-018-04109-8 PMID: 29892050; PubMed Central PMCID: PMC5995836.

137. Yong W, Jiao C, Jianhui W, Yan Z, Qi P, Xiu W, et al. Mono-2-ethyhexyl phthalate advancing the progression of prostate cancer through activating the hedgehog pathway in LNCaP cells. Toxicology in vitro: an international journal published in association with BIBRA. 2016; 32:86–91. Epub 2015/12/30. https://doi.org/10.1016/j.tiv.2015.12.012 PMID: 26710974.

138. Edgar R, Domrachev M, Lash AE. Gene Expression Omnibus: NCBI gene expression and hybridization array data repository. Nucleic acids research. 2002; 30(1):207–10. Epub 2001/12/26. https://doi.org/10.1093/nar/30.1.207 PMID: 11752295; PubMed Central PMCID: PMC99122.

139. Peng H, Shi J, Zhang Y, Zhang H, Liao S, Li W, et al. A novel class of tRNA-derived small RNAs extremely enriched in mature mouse sperm. Cell research. 2012; 22(11):1609–12. Epub 2012/10/10. https://doi.org/10.1038/cr.2012.141 PMID: 23044802; PubMed Central PMCID: PMC3494397.

140. Trapnell C, Roberts A, Goff L, Pertea G, Kim D, Kelley DR, et al. Differential gene and transcript expression analysis of RNA-seq experiments with TopHat and Cufflinks. Nat Protocols. 2012; 7 (3):562–78. https://doi.org/10.1038/nprot.2012.016 PMID: 22383036

141. Ghosh S, Chan CK. Analysis of RNA-Seq Data Using TopHat and Cufflinks. Methods Mol Biol. 2016; 1374:339–61. Epub 2015/11/01. https://doi.org/10.1007/978-1-4939-3167-5_18 PMID: 26519415.

142. Warnes G, Bolker B, Lumley T. gplots: Various R programming tools for plotting data. R package version 2.6.02009 2009.

143. Szklarczyk D, Franceschini A, Wyder S, Forslund K, Heller D, Huerta-Cepas J, et al. STRING v10: protein-protein interaction networks, integrated over the tree of life. Nucleic acids research. 2015; 43 (Database issue):D447–52. Epub 2014/10/30. https://doi.org/10.1093/nar/gku1003 PMID: 25352553; PubMed Central PMCID: PMC4383874.

144. Szklarczyk D, Morris JH, Cook H, Kuhn M, Wyder S, Simonovic M, et al. The STRING database in 2017: quality-controlled protein-protein association networks, made broadly accessible. Nucleic acids research. 2017; 45(D1):D362–D8. Epub 2016/12/08. https://doi.org/10.1093/nar/gkw937 PMID: 27924014; PubMed Central PMCID: PMC5210637.

145. Kulakovskiy IV, Vorontsov IE, Yevshin IS, Sharipov RN, Fedorova AD, Rumynskiy EI, et al. HOCOMOCO: towards a complete collection of transcription factor binding models for human and mouse via large-scale ChIP-Seq analysis. Nucleic acids research. 2017. Epub 2017/11/16. https://doi.org/10.1093/nar/gkx1106 PMID: 29140464.

146. Obenchain V, Lawrence M, Carey V, Gogarten S, Shannon P, Morgan M. VariantAnnotation: a Bioconductor package for exploration and annotation of genetic variants. Bioinformatics. 2014; 30 (14):2076–8. Epub 2014/04/01. https://doi.org/10.1093/bioinformatics/btu168 PMID: 24681907; PubMed Central PMCID: PMC4080743.

147. H. Pagès PA, R. Gentleman, and S. DebRoy Biostrings: Efficient manipulation of biological strings. R package version 2460 2017.

148. Team TBD. BSgenome.Mmusculus.UCSC.mm10: Full genome sequences for Mus Musculus (UCSC version mm10). R package version 140. 2014.

149. Rainer J. EnsDb.Mmusculus.v79: Ensembl based annotation package. R package version 2990 2017.

150. Wasserman WW, Sandelin A. Applied bioinformatics for the identification of regulatory elements. Nature reviews Genetics. 2004; 5(4):276–87. Epub 2004/05/08. https://doi.org/10.1038/nrg1315 PMID: 15131651.

151. Suzuki R, Shimodaira H. Pvclust: an R package for assessing the uncertainty in hierarchical clustering. Bioinformatics. 2006; 22(12):1540–2. Epub 2006/04/06. https://doi.org/10.1093/bioinformatics/btl117 PMID: 16595560.

152. Benjamini Y, Hochberg Y. Controlling the False Discovery Rate: A Practical and Powerful Approach to Multiple Testing. Journal of the Royal Statistical Society Series B (Methodological). 1995; 57(1):289–300.